

# LLM-TS Integrator: Integrating LLM for Enhanced Time Series Modeling

Can (Sam) Chen\*, Gabriel L. Oliveira, Hossein Sharifi-Noghabi, Tristan Sylvain

Borealis AI

## Abstract

Time series (TS) modeling is essential in dynamic systems like weather prediction and anomaly detection. Recent studies utilize Large Language Models (LLMs) for TS modeling, leveraging their powerful pattern recognition capabilities. These methods primarily position LLMs as the predictive backbone, often omitting the mathematical modeling within traditional TS models, such as periodicity. However, disregarding the potential of LLMs also overlooks their pattern recognition capabilities. To address this gap, we introduce *LLM-TS Integrator*, a novel framework that effectively integrates the capabilities of LLMs into traditional TS modeling. Central to this integration is our *mutual information* module. The core of this *mutual information* module is a traditional TS model enhanced with LLM-derived insights for improved predictive abilities. This enhancement is achieved by maximizing the mutual information between traditional model’s TS representations and LLM’s textual representation counterparts, bridging the two modalities. Moreover, we recognize that samples vary in importance for two losses: traditional prediction and mutual information maximization. To address this variability, we introduce the *sample reweighting* module to improve information utilization. This module assigns dual weights to each sample: one for prediction loss and another for mutual information loss, dynamically optimizing these weights via bi-level optimization. Our method achieves state-of-the-art or comparable performance across five mainstream TS tasks, including short-term and long-term forecasting, imputation, classification, and anomaly detection.

## 1 Introduction

Time series (TS) modeling, as emphasized in (Hyndman and Athanasopoulos 2018), is crucial for a variety of real-world applications. It is instrumental in forecasting meteorological factors for weather prediction (Wu et al. 2021), imputing missing data in economic TS (Friedman 1962), detecting anomalies in industrial monitoring data for maintenance (Gao et al. 2020), and classifying trajectories for action recognition (Franceschi, Dieuleveut, and Jaggi 2019). Given its significant practical impact, TS analysis continues to attract substantial attention (Lim and Zohren 2021; Wen et al. 2022).

Recent efforts in TS modeling have increasingly adopted Large Language Models (LLMs) to leverage their exceptional

pattern recognition capabilities (Jiang et al. 2024; Zhou et al. 2024b; Jin et al. 2024; Sun et al. 2023; Gruver et al. 2024; Cao et al. 2024). While these innovative approaches validate the potential of LLMs in TS modeling, they primarily position LLMs as the core predictive model. Consequently, they often omit the mathematical modeling tailored specifically for TS models, such as employing the Fourier Transform to capture periodic patterns (Wu et al. 2023).

On the other hand, fully disregarding the potential of LLMs also overlooks their powerful pattern recognition capabilities. It is important to recognize the balance between leveraging LLMs for their advanced capabilities and utilizing traditional TS models for their mathematical modeling, to enhance the overall performance and accuracy of TS predictions. In response, we propose *LLM-TS Integrator*, a novel framework that effectively integrates the capabilities of LLMs into traditional TS modeling.

Central to our framework is a *mutual information* module, as depicted in Figure 1(a). The core of this module is a traditional predictive model, which we enhance with insights derived from LLMs to improve its predictive abilities. In this work, we primarily utilize TimesNet (Wu et al. 2023) as the traditional predictive model due to its exceptional performance and insight into periodic modeling, and our framework is also applicable to other traditional TS models (see in Section 4.6). We achieve this enhancement by maximizing the mutual information (Sun et al. 2019) between the TS representations from traditional models and their textual counterparts from LLMs, thereby bridging these two modalities. Despite its established use, mutual information maximization has not been previously applied to the intersection of TS and text domain. With textual descriptions often missing from TS data, we propose generating such descriptions via a carefully designed template. This template is enriched with essential background and statistical details pertinent to the TS, thereby enriching the LLM’s comprehension of the TS context.

Our first module introduces a dual loss framework: traditional prediction and mutual information, and we recognize that the importance of samples differs between the two losses. For instance, a large prediction loss for a sample highlights its learning potential, emphasizing the need to focus on its prediction loss. This scenario also implies that the model’s learning for this sample is inadequate and its hidden representation is suboptimal for mutual information computation.

\*Work done during an internship at Borealis AI. Preprint. Under review.

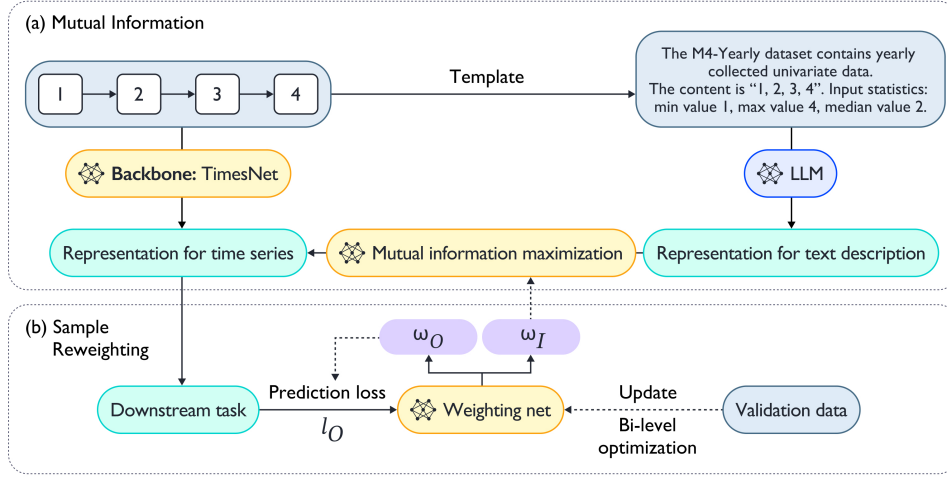


Figure 1: Illustration of *LLM-TS Integrator*. Module (a) enhances the traditional TS model (TimesNet) with LLM-derived insights by mutual information maximization. Module (b) optimizes sample importance for both prediction loss and mutual information loss to improve information utilization.

Consequently, the sample’s contribution to the mutual information calculation should be reduced. To manage this variability, we have introduced a novel *sample reweighting* module powered by a simple MLP (multilayer perceptron) network, as depicted in Figure 1(b). This module processes the sample prediction loss to produce dual weights for each sample, one for the prediction loss and another for the mutual information loss. These weights are optimized through bi-level optimization, thereby enhancing the efficacy of information utilization.

Our primary contributions are as follows:

- We introduce *LLM-TS Integrator*, which consists of *mutual information* and *sample reweighting*. The first module enhances traditional TS modeling with capabilities from LLMs through mutual information maximization.
- The second module optimizes sample importance for both prediction loss and mutual information loss, which improves information utilization.
- Extensive experiments across five mainstream TS tasks—short-term and long-term forecasting, imputation, classification, and anomaly detection—demonstrate the effectiveness of our framework.

## 2 Preliminaries

**TimesNet.** In this paper, we mainly choose TimesNet as the traditional predictive model due to its exceptional performance (Wu et al. 2023) and also explore other additional traditional models including ETSformer (Woo et al. 2022), Stationary (Liu et al. 2022), and FreTS (Yi et al. 2024) in Section 4.6. Previous studies to modeling temporal variations in 1D time series often struggle with complex temporal patterns. TimesNet addresses this challenge by decomposing these complex variations into multiple intra-period and inter-period variations. This is achieved by transforming the 1D time series into a series of 2D tensors, each corresponding to

different periods. For the time series  $x$ , we derive its representation  $h_{\theta}^m(x)$  using the TimesNet model parameterized by  $\theta$  where  $m$  represents *model*.

**Large Language Models.** Language models are trained on extensive collections of natural language sequences, with each sequence consisting of multiple tokens. Notable large language models such as GPT-3 (Brown et al. 2020) and Llama2 (Touvron et al. 2023) aim to predict the next token based on preceding tokens, demonstrating their capabilities through improvements in model parameter size and the amount of training data. Each language model uses a tokenizer that breaks down an input string into a sequence of recognizable tokens. However, the training of current large language models is solely focused on natural language, not encompassing time series data. This limitation presents challenges for the direct application of large language models to time series analysis.

## 3 Method

In this section, we present the *LLM-TS Integrator* framework, which effectively integrates the capabilities of LLMs into traditional TS modeling. This framework consists of two modules: *mutual information* and *sample reweighting*. The first module enhances a traditional TS model with LLM-derived insights for improved predictive abilities, as explored in Section 3.1. The second module optimizes weights for prediction loss and mutual information loss via bi-level optimization, improving information utilization, as covered in Section 3.2. The overall algorithm is shown in Algorithm 1.

### 3.1 Mutual Information

Previous studies (Zhou et al. 2024b; Jin et al. 2023) have predominantly highlighted the use of Large Language Models (LLMs) as the core predictive model in the TS analysis, often omitting the mathematical modeling within traditional TS models, such as periodicity.

---

**Algorithm 1: LLM-TS Integrator**

---

**Input:** The TS dataset  $\mathcal{D}$ , number of training iterations  $T$ .

**Output:** Trained TS model parameterized by  $\theta^*$ .

- 1: */\* Mutual Information Module \*/*
  - 2: Train a traditional TS model (e.g., TimesNet) parameterized by  $\theta$  using  $\mathcal{D}$ .
  - 3: Generate text description  $t$  for TS sample  $x$  via a designed template.
  - 4: Derive hidden representations  $h_{\theta}^m(x)$  from the TS model and  $h^l(t)$  from the LLM.
  - 5: **while**  $\tau \leq T - 1$  **do**
  - 6:   Sample  $x, t, y$  from  $\mathcal{D}$ , where  $y$  are the labels.
  - 7:   Optimize a discriminator model  $T_{\beta}$  to estimate mutual information as per Eq. (2).
  - 8:   */\* Sample Reweighting Module \*/*
  - 9:   Process sample loss  $l_O$  with the weighting net to produce dual weights as per Eq. (3), (4).
  - 10:   Adopt bi-level optimization to update the weighting net following Eq. (6), (7).
  - 11:   Re-calculate dual weights using the updated weighting net per Eq. (3), (4).
  - 12:   Calculate the overall loss to update the TS model as per Eq. (5).
  - 13: **end while**
  - 14: Return the trained TS model parameterized by  $\theta^*$ .
- 

In contrast, our framework utilizes a traditional TS model as the predictive backbone, enhanced by the advanced capabilities of LLMs. In this paper, we employ TimesNet, as outlined in Section 2, as the traditional predictive model, and we further examine other models in Section 4.6. This hybrid methodology combines the advantages of both traditional TS models and modern LLMs. We achieve this integration via a *mutual information* module, which maximizes the mutual information between the TS data representations derived from the traditional model and their corresponding textual representations derived from LLMs.

**Mutual Information Estimation.** Estimating the mutual information between hidden representations of a time series (TS) sample  $x$  and its corresponding textual description  $t$  is essential. For the TS sample  $x$ , we derive its representation  $h_{\theta}^m(x)$  using TimesNet, a model parameterized by  $\theta$ . For the text  $t$ , its representation  $h^l(t)$  is extracted using a pre-trained Large Language Model (LLM), where  $l$  denotes the language model. In this study, we employ the LLaMA-3b model (Touvron et al. 2023) as our primary LLM, while also evaluating other LLMs as detailed in Section 4.6.

We estimate mutual information using the Jensen-Shannon MI estimator (Sun et al. 2019; Nowozin, Cseke, and Tomioka 2016) and additionally explore the MINE estimator (Hjelm et al. 2018) as detailed in Appendix B.12. Specifically, let  $(x, t)$  represent a sample from the TS set  $\mathbb{S}$ , and  $(\tilde{x}, \tilde{t})$  denote a sample from  $\tilde{\mathbb{S}} = \mathbb{S}$  where  $(x, t) \neq (\tilde{x}, \tilde{t})$ . Within this context,  $\mathbb{S}$  denotes the TS training distribution while the product  $\mathbb{S} \times \tilde{\mathbb{S}}$  represents pairs of distinct samples within  $\mathbb{S}$ . Then the

lower bound of mutual information can be estimated as:

$$I(\theta, \beta) = \mathbb{E}_{\mathbb{S}}[-sp(-T_{\beta}(h_{\theta}^m(x), h^l(t)))] - \mathbb{E}_{\mathbb{S} \times \tilde{\mathbb{S}}}[sp(T_{\beta}(h_{\theta}^m(x), h^l(\tilde{t})))] \quad (1)$$

where  $T_{\beta}$  denotes the discriminator parameterized by  $\beta$  and  $sp$  is the softplus function. For the details of  $T_{\beta}$ , we feed the positive and negative examples into a 1-layered fully-connected network, and then output the dotproduct of the two representations. The mutual information estimation begins by fixing the model parameters  $\theta$ , followed by training  $\beta$  as the estimator. Specifically, we optimize  $\beta$  via the following:

$$\hat{\beta} = \beta - \eta_0 \cdot \frac{\partial I(\theta, \beta)}{\partial \beta} \quad (2)$$

where  $\eta_0$  denotes the learning rate. Subsequently, we refine the model parameters  $\theta$  to maximize mutual information, thereby enriching the traditional TS model with insights derived from LLMs. This alternating optimization procedure between model and discriminator is repeated each epoch.

**Text Description for Time Series.** In our approach, we assume each time series (TS) sample  $x$  is paired with a corresponding textual description,  $t$ . However, textual descriptions are frequently unavailable for many TS datasets. To bridge this gap, we introduce a methodology for generating textual descriptions of TS data. We propose creating textual representations that capture essential background and statistical details of the TS inspired by (Jin et al. 2023). This process can be systematically implemented using the following carefully designed template:

```
template = (  
    "{task_description}. The content is: {TS}." "  
    "Input statistics:  
    min value {min(TS)}, max value {max(TS)}, "  
    "median value {median(TS)},  
    top 5 lags {compute_lags(TS)}."  
)
```

## 3.2 Sample Reweighting

Our *mutual information* module introduces two distinct loss functions: (1) the original sample prediction loss,  $l_O(x, y)$ , hereafter referred to as  $l_O$ , which corresponds to the prediction loss for a TS sample  $x$  and its label  $y$ , and (2) the mutual information maximization loss, denoted as  $-I(\theta, \beta)$ . We acknowledge that the significance of samples varies between these two losses. Specifically, a large prediction loss  $l_O$  indicates a sample’s substantial learning potential, thereby justifying a higher weight  $\omega_O$  for its prediction loss. Conversely, this suggests that the sample’s representation may be suboptimal for mutual information computation, warranting a lower weight  $\omega_I$ .

To address this disparity, we have developed a novel *sample reweighting* module, described as follows.

**Weighting Network.** To automate weight assignment, our module employs a two-layer MLP network parameterized by  $\alpha$ , which processes the sample prediction loss to produce a pair of weights:

$$\omega_O(\alpha), \omega_I(\alpha) = MLP_{\alpha}(l_O) \quad (3)$$

This process involves converting the sample loss  $l_O$  into a latent code  $z$  through a hidden layer. The network then outputs dual weights:

$$\omega_O(\alpha), \omega_I(\alpha) = \sigma(m_O \cdot z), \sigma(m_I \cdot z) \quad (4)$$

where  $m_O > 0$  and  $m_I < 0$  to ensure a negative correlation between  $\omega_O$  and  $\omega_I$ . The function  $\sigma(\cdot)$  denotes sigmoid.

For a batch of  $N$  samples, the weight vector  $\omega_O(\alpha) \in \mathbb{R}^N$  is directly applied to the original prediction loss vector  $l_O \in \mathbb{R}^N$ , resulting in the weighted average loss calculated as  $\text{mean}(\omega_O(\alpha) \cdot l_O)$ . Similarly, the weight vector  $\omega_I(\alpha) \in \mathbb{R}^N$  not only reflects the overall significance of the mutual information but also each sample’s individual contribution to this metric. The mean of these weights  $\text{mean}(\omega_I(\alpha))$  represents the overall importance. For mutual information computations,  $\omega_I(\alpha)$  is transformed into a probability distribution  $p_I^i = \frac{\omega_I^i}{\sum_{i=1}^N \omega_I^i}$ . This adjustment affects the distribution used in mutual information calculations, necessitating a recalculation of mutual information as  $I(\theta, \beta, \alpha)$ , with details provided in Appendix B.1. As a result, the overall loss is formulated as:

$$\begin{aligned} \mathcal{L}(\theta, \alpha) = & \text{mean}(\omega_O(\alpha) \cdot l_O) \\ & + \text{mean}(\omega_I(\alpha)) \cdot [-I(\theta, \beta, \omega_I(\alpha))] \end{aligned} \quad (5)$$

**Bi-level Optimization.** The ensuing challenge is optimizing the weighting network  $\alpha$ . We achieve this by leveraging the supervision signals from a small validation dataset (Chen et al. 2022). If the weighting network is properly optimized, the model trained with these weights is expected to show improved performance on the validation dataset in terms of the validation loss  $\mathcal{L}_V(\theta) = \frac{1}{M} \sum_j^M l_O^j(x_j, y_j)$ , where  $M$  denotes the size of the validation set. This constitutes a bi-level optimization problem. At the inner level, model training is conducted through gradient descent:

$$\hat{\theta}(\alpha) = \theta - \eta_1 \cdot \frac{\partial \mathcal{L}(\theta, \alpha)}{\partial \theta} \quad (6)$$

The objective is to ensure that the model performs optimally on the validation dataset:

$$\hat{\alpha} = \alpha - \eta_2 \cdot \frac{\partial \mathcal{L}_V(\theta(\alpha))}{\partial \alpha} \quad (7)$$

Both  $\eta_1$  and  $\eta_2$  represent the learning rates for the respective optimization steps. Through the minimization of the validation loss, we aim to optimize the weighting network  $\alpha$ .

## 4 Experimental Results

To demonstrate the versatility of our *LLM-TS Integrator*, we conduct extensive experiments across five main tasks: short- and long-term forecasting, imputation, classification, and anomaly detection. To maintain experimental integrity, our methodology adheres to the setup in (Wu et al. 2023). We detail the experimental setting in Appendix B.2.

**Baselines.** Our evaluation employs a comprehensive array of baseline models across several architectural designs (1) CNN-based models, specifically TimesNet (Wu et al. 2023); (2) MLP-based models, including LightTS (Zhang

et al. 2022) and DLinear (Zeng et al. 2023); (3) Transformer-based models, such as Reformer (Kitaev, Kaiser, and Levskaya 2020), Informer (Zhou et al. 2021a), Autoformer (Wu et al. 2021), FEDformer (Zhou et al. 2022), Nonstationary Transformer (Liu et al. 2022), ETSformer (Woo et al. 2022), and PatchTST (Nie et al. 2022); (4) LLM-based models, represented by GPT4TS (Zhou et al. 2024b). While we assess a wide range of models, we focus our discussion on the top-performing ones as highlighted in (Zhou et al. 2024b).

Additional comparisons for forecasting tasks include LLM-based models like Time-LLM (Jin et al. 2023) and TEST (Sun et al. 2023). For short-term forecasting, models like N-HiTS (Challu et al. 2023) and N-BEATS (Oreshkin et al. 2019) are included. Anomaly detection tasks are assessed using Anomaly Transformer (Xu et al. 2021), and for classification tasks, models such as XGBoost (Chen and Guestrin 2016), Rocket (Dempster, Petitjean, and Webb 2020), LST-Net (Lai et al. 2018), LSSL (Gu, Goel, and Ré 2021), Pyraformer (Liu et al. 2021), TCN (Franceschi, Dieuleveut, and Jaggi 2019), and Flowformer (Huang et al. 2022) are considered. This broad selection of baselines enables a rigorous and fair comparison across various tasks, highlighting the capabilities of our method.

### 4.1 Main Results

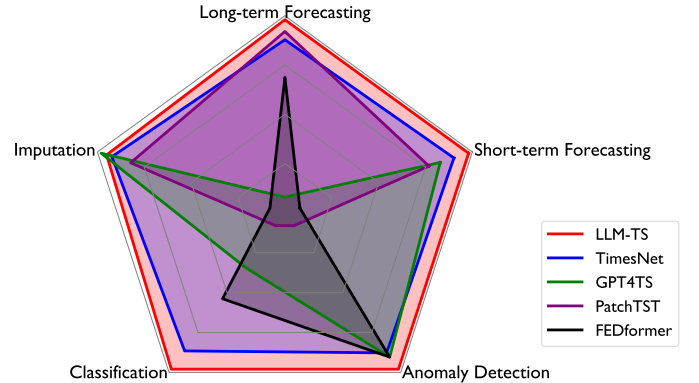


Figure 2: Model performance across different tasks.

Figure 2 demonstrates that our *LLM-TS Integrator* consistently outperforms other methods in various tasks, underscoring its efficacy. We will refer to our method as *LLM-TS* in the tables for brevity. Unless otherwise indicated, we cite results from TimesNet (Wu et al. 2023). We reproduce TimesNet and GPT4TS (Zhou et al. 2024b) experiments for all tasks. All results are averages from three runs with different seeds. Standard deviations for ablation studies are detailed in Appendix 8. The best results are highlighted in bold, with the second-best underlined. We also (1) present several show-cases of our method in Appendix B.4 and (2) discuss the model efficiency in Appendix B.6

### 4.2 Short- and Long- Term Forecasting

**Setup.** To comprehensively assess our framework’s forecasting capabilities, we engage it in both short- and long-

term forecasting settings. In the realm of short-term forecasting, we utilize the M4 dataset (Spyros Makridakis 2018), which aggregates univariate marketing data on a yearly, quarterly, and monthly basis. For long-term forecasting, we examine five datasets following (Zhou et al. 2024b): ETT (Zhou et al. 2021b), Electricity (UCI 2015), Traffic (PeMS 2024), Weather (Wetterstation 2024), and ILI (CDC 2024). We adhere to the TimesNet setting with an input length of 96. For LLM-based methods like GPT4TS and Time-LLM, which use different input lengths, we rerun the experiments using their code. For PatchTST, we cite the results from (Wang et al. 2023), as the original PatchTST uses an input length of 512. Due to shorter input lengths in this study compared to the original, the reported performance is lower.

**Results.** As shown in Tables 1 and 2, our *LLM-TS* performs exceptionally well in both short- and long-term settings. It consistently surpasses TimesNet, highlighting the effectiveness of incorporating LLM-derived insights. Furthermore, it generally outperforms other LLM-based methods such as GPT4TS, TIME-LLM, and TEST, underscoring the advantages of integrating traditional TS modeling.

### 4.3 Imputation

**Setup.** To assess our method’s imputation capabilities, we employ three datasets: ETT (Zhou et al. 2021b), Electricity (UCI 2015), and Weather (Wetterstation 2024), serving as our benchmarks. To simulate various degrees of missing data, we randomly obscure time points at proportions of {12.5%, 25%, 37.5%, 50%} following (Wu et al. 2023).

**Results.** Table 3 illustrates that our method achieves performance comparable to GPT4TS and surpasses other baselines, highlighting its effectiveness. We attribute the robust performance of GPT4TS primarily to its backbone feature extractor: the pre-trained language model, which excels at capturing time series patterns, enhancing its imputation proficiency.

### 4.4 Classification

**Setup.** We focus on the application of our method to sequence-level time series classification tasks, a crucial test of its ability to learn high-level representations from data. Specifically, we employ 10 diverse multivariate datasets sourced from the UEA Time Series Classification repository (Bagnall et al. 2018). These datasets encompass a wide range of real-world applications, including gesture and action recognition, audio processing, medical diagnosis, among other practical domains. We reproduce the results of TEST based on their code (Sun et al. 2023).

**Results.** As depicted in Figure 3, our *LLM-TS Integrator* achieves superior performance with an average accuracy of 73.4%. As detailed in Appendix B.10, it consistently outperforms other LLM-based methods across most tasks, including GPT4TS and TEST. We attribute this enhanced capability to the traditional TS modeling techniques in our framework, which effectively capture classification characteristics more adeptly than LLMs.

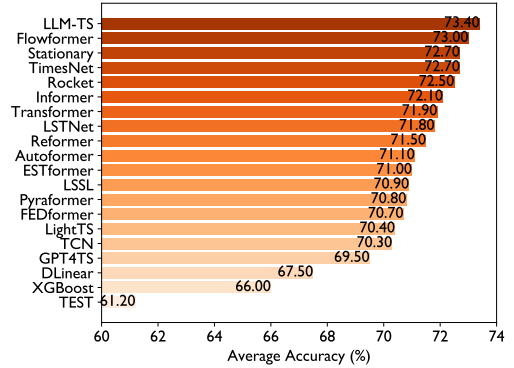


Figure 3: Model comparison in classification.

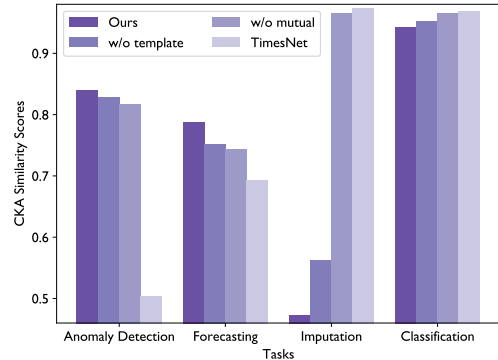


Figure 4: CKA by Task.

### 4.5 Anomaly Detection

**Setup.** Our study concentrates on unsupervised time series anomaly detection, aiming to identify aberrant time points indicative of potential issues. We benchmark our method against five established anomaly detection datasets: SMD (Su et al. 2019), MSL (Hundman et al. 2018), SMAP (Hundman et al. 2018), SWaT (Mathur and Tippenhauer 2016), and PSM (Abdulaal, Liu, and Lancewicki 2021). These datasets span a variety of applications, including service monitoring, space and earth exploration, and water treatment processes. For a consistent evaluation framework across all experiments, we employ the classical reconstruction error metric to determine anomalies following (Wu et al. 2023).

**Results.** As indicated in Table 4, our *LLM-TS Integrator* exhibits superior performance with an average F1-score of 85.17%. This result underscores the versatility of *LLM-TS*, demonstrating its capability not only in classifying complete sequences, as discussed previously, but also in effectively detecting anomalies in time series data.

### 4.6 Ablations

In this section, we first verify the effectiveness of our framework by sequentially removing key components: (1) *mutual information* module and (2) *sample reweighting* module. Additionally, for *mutual information*, we explore the impact of removing the template while retaining the raw time series data inputs to the LLM. We denote these variants as *w/o*

Table 1: Short-term M4 forecasting. The prediction lengths are in [6, 48] and results are obtained by weighting averages across multiple datasets with varying sampling intervals. Full results are in Appendix B.7.

Methods	LLM-TS	TimesNet	GPT4TS	TIME-LLM	TEST	PatchTST	N-HiTS	N-BEATS	FEDformer	Stationary	Autoformer
SMAPE	<b>11.819</b>	11.908	11.991	11.983	11.927	12.059	11.927	<u>11.851</u>	12.840	12.780	12.909
MASE	<b>1.588</b>	1.612	1.600	<u>1.595</u>	1.613	1.623	1.613	1.599	1.701	1.756	1.771
OWA	<b>0.851</b>	0.860	0.861	0.859	0.861	0.869	0.861	<u>0.855</u>	0.918	0.930	0.939

Table 2: Long-term forecasting: Averages over 4 lengths: 24, 36, 48, 60 for ILI, and 96, 192, 336, 720 for others. Full results in Appendix B.8.

Methods	LLM-TS		TimesNet		TIME-LLM		DLinear		PatchTST		GPT4TS		FEDformer		TEST		Stationary		ETSformer	
	MSE	MAE	MSE	MAE	MSE	MAE	MSE	MAE	MSE	MAE	MSE	MAE	MSE	MAE	MSE	MAE	MSE	MAE	MSE	MAE
Weather	<b>0.257</b>	<b>0.285</b>	<u>0.265</u>	0.290	0.279	0.296	<u>0.265</u>	0.317	<u>0.265</u>	<b>0.285</b>	0.275	0.292	0.309	0.360	0.291	0.315	0.288	0.314	0.271	0.334
ETTh1	0.454	<b>0.451</b>	0.470	0.462	0.474	0.459	0.456	0.452	0.516	0.484	<b>0.473</b>	<b>0.451</b>	<b>0.440</b>	0.460	<b>0.440</b>	0.460	0.570	0.537	0.542	0.510
ETTh2	0.396	<u>0.413</u>	0.413	0.426	0.398	0.415	0.559	0.515	<u>0.391</u>	<b>0.411</b>	<b>0.383</b>	0.410	0.437	0.449	0.414	0.432	0.526	0.516	0.439	0.452
ETTM1	<b>0.401</b>	0.409	0.414	0.418	0.437	0.421	0.403	<u>0.407</u>	0.406	0.407	0.408	<b>0.400</b>	0.448	0.452	<u>0.402</u>	0.411	0.481	0.456	0.429	0.425
ETTM2	0.295	<b>0.331</b>	0.294	<b>0.331</b>	0.298	0.342	0.350	0.401	<b>0.290</b>	0.334	<b>0.290</b>	0.335	0.305	0.349	0.323	0.359	0.306	0.347	0.293	0.342
ILI	<b>1.973</b>	<b>0.894</b>	2.266	0.974	2.726	1.098	2.616	1.090	2.184	<u>0.906</u>	5.117	1.650	2.847	1.144	3.324	1.232	<u>2.077</u>	0.914	2.497	1.004
ECL	<u>0.194</u>	0.299	0.198	<u>0.298</u>	0.229	0.315	0.212	0.300	0.216	0.318	0.206	<b>0.285</b>	0.214	0.327	0.237	0.324	<b>0.193</b>	0.296	0.208	0.323
Traffic	0.618	<b>0.333</b>	<u>0.627</u>	<u>0.335</u>	0.606	0.395	0.625	0.383	<b>0.529</b>	0.341	<u>0.561</u>	0.373	0.610	0.376	0.581	0.388	0.624	<u>0.340</u>	0.621	0.396
Average	<b>0.574</b>	<b>0.427</b>	0.618	0.442	0.681	0.468	0.686	0.483	<u>0.600</u>	<u>0.436</u>	0.964	0.525	0.701	0.489	0.756	0.491	0.633	0.465	0.662	0.473

*mutual*, *w/o reweight* and *w/o template*. Our experiments span long-term forecasting tasks including Weather, ETTh1, ETTh2, ETTm1 and ILI. As detailed in Table 5, the removal of any component leads to a decrease in performance, confirming the value of each design element. Additionally, we explore the use of the MINE estimator (Hjelm et al. 2018) instead of the Jensen-Shannon MI estimator in our main paper, with further details provided in Appendix B.12. Lastly, we showcase various case studies to demonstrate the enhancements facilitated by our method in Appendix B.4 and explore template variations in Appendix B.5.

**Mutual Information.** We further explore the *mutual information* module from a representation learning perspective, following the findings in (Wu et al. 2023). They adopt a CKA (Centered Kernel Alignment) metric which measures similarity between representations obtained from the first and last layer of a model and they find that forecasting and anomaly detection benefits from high CKA similarity, contrasting with that imputation and classification tasks benefits from lower CKA similarity.

Experiments are conducted using the MSL dataset for the anomaly detection task, the Weather dataset for forecasting, the ETTh1 dataset for imputation, and the PEMS-SF dataset for classification. As depicted in Figure 4, the removal of components in our method results in decreased CKA similarity in anomaly detection and forecasting tasks, but an increase in imputation and classification tasks. This observation further substantiates the effectiveness of our components.

**Sample Reweighting.** Regarding the *sample reweighting* module, we illustrate the behavior of the learned weighting network in Appendix B.12. The trend confirms our hypothesis: sample weight  $\omega_O$  increases with the prediction loss  $l_O$ , and weight  $\omega_I$  decreases as  $l_O$  increases. This pattern validates our *sample reweighting* module. Further discussion comparing this module to a fixed weight scheme are presented in Appendix B.12.

To verify the effectiveness of our method, we conduct ablation studies focusing on (1) traditional time series (TS) models and (2) language models.

**Traditional Models.** Although we utilize TimesNet as our primary model, our framework is applicable to other traditional models. We explored additional traditional models including ETSformer (Woo et al. 2022), Stationary (Liu et al. 2022), and FreTS (Yi et al. 2024). As shown in Table 6, integrating *LLM-TS* generally enhances performance across all traditional models, underscoring the benefits of our method.

**Language Models.** In the main paper, the LLaMA-3b model (Touvron et al. 2023) is used to generate embeddings for the TS language description. We compare it with GPT2 (Radford et al. 2019) and BERT (Devlin et al. 2018) to assess different embeddings’ performance. Table 7 reveals that LLaMA-3b generally outperforms the alternatives, and all LMs improve results compared to non-LLM approaches, validating the effectiveness of *LLM-TS Integrator*.

## 5 Related Work

**LLM for TS Modeling.** FPT (Zhou et al. 2024b) suggests utilizing pre-trained language models to extract features from time series for improved predictions. TIME-LLM (Jin et al. 2024) and TEST (Sun et al. 2023) adapt LLMs for general time series forecasting by maintaining the original language model structure while reprogramming the input to fit time series data (Zhou et al. 2024a). LLMTIME (Gruver et al. 2024) interprets time series as sequences of numbers, treating forecasting as a next-token prediction task akin to text processing, applying pre-trained LLMs for this purpose. Given that it is not a state-of-the-art method and primarily targets zero-shot forecasting, it has not been incorporated into our experimental framework. TEMPO (Cao et al. 2024) utilizes essential inductive biases of the TS task for generative pre-trained transformer models.

**Time Series to Text.** PromptCast (Xue and Salim 2023) proposes to transform the numerical input and output into prompts, which enables forecasting in a sentence-to-sentence manner. Time-LLM (Jin et al. 2024) incorporates background, instruction and statistical information of the time series data via natural language to facilitate time series forecasting in LLM. LLMTIME (Gruver et al. 2023) converts time series

Table 3: Imputation task: Randomly masked {12.5%, 25%, 37.5%, 50%} of points in 96-length series, averaging results over 4 mask ratios. Full results are in Appendix B.9.

Methods	LLM-TS		TimesNet		GPT4TS		PatchTST		LightTS		DLinear		FEDformer		Stationary		Autoformer		Reformer	
	MSE	MAE	MSE	MAE	MSE	MAE	MSE	MAE	MSE	MAE	MSE	MAE	MSE	MAE	MSE	MAE	MSE	MAE	MSE	MAE
ETM1	<b>0.025</b>	<b>0.103</b>	0.028	0.109	0.028	0.108	0.047	0.140	0.104	0.218	0.093	0.206	0.062	0.177	0.036	0.126	0.051	0.150	0.055	0.166
ETM2	<b>0.021</b>	<b>0.087</b>	0.022	0.089	0.023	0.088	0.029	0.102	0.046	0.151	0.096	0.208	0.101	0.215	0.026	0.099	0.029	0.105	0.157	0.280
ETTh1	0.087	0.198	0.090	0.199	<b>0.069</b>	<b>0.174</b>	0.115	0.224	0.284	0.373	0.201	0.306	0.117	0.246	0.094	0.201	0.103	0.214	0.122	0.245
ETTh2	<b>0.050</b>	0.148	0.051	0.150	<b>0.050</b>	<b>0.144</b>	0.065	0.163	0.119	0.250	0.142	0.259	0.163	0.279	0.053	0.152	0.055	0.156	0.234	0.352
ECL	0.094	0.211	0.095	0.212	<u>0.091</u>	<u>0.207</u>	<b>0.072</b>	<b>0.183</b>	0.131	0.262	0.132	0.260	0.130	0.259	0.100	0.218	0.101	0.225	0.200	0.313
Weather	<b>0.030</b>	<b>0.056</b>	<u>0.031</u>	0.059	0.032	0.058	0.034	<b>0.055</b>	0.055	0.117	0.052	0.110	0.099	0.203	0.032	0.059	<u>0.031</u>	0.057	0.038	0.087
Average	<u>0.051</u>	<u>0.134</u>	0.053	0.136	<b>0.049</b>	<b>0.130</b>	0.060	0.144	0.123	0.228	0.119	0.224	0.112	0.229	0.056	0.142	0.061	0.151	0.134	0.240

Table 4: Anomaly detection task. F1-score (as %). \*. in the Transformers represents the name of \*former. Full results are in Appendix B.11.

Methods	LLM-TS	TimesNet	GPT4TS	PatchTS.	ETS.	FED.	LightTS	DLinear	Stationary	Auto.	Pyra.	Anomaly.**	In.	Re.	Trans.
SMD	84.69	84.57	84.32	84.62	83.13	85.08	82.53	77.10	84.72	85.11	83.04	85.49	81.65	75.32	79.56
MSL	81.11	80.34	81.73	78.70	85.03	78.57	78.95	84.88	77.50	79.05	84.86	83.31	84.06	84.40	78.68
SMAP	69.41	69.18	68.86	68.82	69.50	70.76	69.21	69.26	71.09	71.12	71.09	71.18	69.92	70.40	69.70
SWaT	93.23	93.12	92.59	85.72	84.91	93.19	93.33	87.52	79.88	92.74	91.78	83.10	81.43	82.80	80.37
PSM	97.43	97.27	97.34	96.08	91.76	97.23	97.15	93.55	97.29	93.29	82.08	79.40	77.10	73.61	76.07
Average	<b>85.17</b>	84.90	<u>84.97</u>	82.79	82.87	84.97	84.23	82.46	82.08	84.26	82.57	80.50	78.83	77.31	76.88

Table 5: Results averaged over 4 prediction lengths.

Methods	Ours		w/o mutual		w/o template		w/o reweight		TimesNet	
	MSE	MAE	MSE	MAE	MSE	MAE	MSE	MAE	MSE	MAE
Weather	<b>0.257</b>	<b>0.285</b>	0.264	0.290	0.263	0.288	0.264	0.291	0.265	0.290
ETTh1	<b>0.454</b>	<b>0.451</b>	0.467	0.460	0.465	0.460	0.464	0.463	0.470	0.462
ETM1	<b>0.401</b>	<b>0.409</b>	0.411	0.417	0.406	0.415	0.403	0.411	0.414	0.418
ILI	<b>1.973</b>	<b>0.894</b>	2.221	0.942	2.173	0.950	2.173	0.947	2.266	0.974

Table 6: Ablation results on different traditional models. Full results are in Appendix B.12.

Methods	ETSformer		ETS LLM-TS		Stationary		Stat LLM-TS		FreTS		FreTS LLM-TS	
	MSE	MAE	MSE	MAE	MSE	MAE	MSE	MAE	MSE	MAE	MSE	MAE
Weather	0.313	0.382	0.307	0.375	0.282	0.307	0.284	0.309	0.262	0.306	0.255	0.302
ETTh1	0.799	0.684	0.791	0.678	0.667	0.582	0.653	0.572	0.484	0.473	0.478	0.466
ETM1	0.638	0.583	0.555	0.528	0.527	0.477	0.522	0.471	0.415	0.422	0.407	0.415
ILI	3.922	1.367	3.740	1.320	2.722	1.041	2.205	0.935	3.449	1.279	3.158	1.211

data into a string of numbers and predicts future values as if completing a text.

**Mutual Information** The Infomax principle (Linsker 1988; Bell and Sejnowski 1995), applied in the context of neural networks, advocates for maximizing mutual information between the inputs and outputs of a network. Traditionally, quantifying mutual information was challenging outside a few specific probability distributions, as discussed in (Shwartz-Ziv and Tishby 2017). This complexity led to the development of various heuristics and approximations (Tishby, Pereira, and Bialek 2000). More recently, a breakthrough came with MINE (Belghazi et al. 2021), which introduced a neural estimator capable of assessing mutual information between two arbitrary quantities with a precision that depends on the capacity of the encoding network. This

Table 7: Ablation results on different LLM embeddings. Full results are in Appendix B.12.

Methods	LLM-TS (LLaMA)		LLaMA w/o template		GPT2		BERT		No LLM	
	MSE	MAE	MSE	MAE	MSE	MAE	MSE	MAE	MSE	MAE
Weather	<b>0.257</b>	<b>0.285</b>	0.263	0.288	0.261	0.287	0.260	0.287	0.264	0.290
ETTh1	<b>0.454</b>	<b>0.451</b>	0.465	0.460	0.464	0.458	0.467	0.460	0.467	0.460
ETM1	<b>0.401</b>	<b>0.409</b>	0.406	0.415	0.406	0.413	0.406	0.412	0.411	0.417
ILI	<b>1.973</b>	<b>0.894</b>	2.173	0.950	2.169	0.936	2.193	0.952	2.221	0.942

innovative approach has spearheaded advancements in the field of representation learning (Hjelm et al. 2019; Sylvain, Petrini, and Hjelm 2019). The estimator we utilize is based on the Jensen-Shannon divergence variant of the MINE mutual information estimator.

**Sample Reweighting.** Sample reweighting is commonly used to improve training efficacy (Fang et al. 2024; Wang et al. 2024; Yuan et al. 2024a; Zhang et al. 2024; Yuan et al. 2024b). Traditional approaches (Freund and Schapire 1997; Sun et al. 2007) assign larger weights to samples with higher loss values, as these hard samples have greater learning potential. Recent studies (Ren et al. 2018) suggest using a validation set to guide the learning of sample weights, which can enhance model training. Notably, meta-weight-net (Shu et al. 2019) proposes learning a mapping from sample loss to sample weight. In this work, we adopt an MLP network that takes sample prediction loss as input and outputs dual weights for prediction loss and mutual information loss.

## 6 Conclusion and Discussion

In conclusion, the *LLM-TS Integrator framework* offers a promising approach to integrating Large Language Models (LLMs) with traditional TS methods. This work extends our prior findings from the workshop (Chen et al. 2024). By encouraging high mutual information between textual and TS data, our method aims to maintain the distinct characteristics of TS while benefiting from the advanced pattern recognition capabilities of LLMs. The introduced sample reweighting module enhances performance by dynamically adjusting the relevance of each sample based on its predictive and informational contributions. Comprehensive empirical evaluations suggest that this framework improves accuracy across various TS tasks, including forecasting, anomaly detection, and classification. However, further research is necessary to confirm these results across more diverse datasets and to explore additional LLM features that could further enrich our model. Additionally, it is important to acknowledge current limitations, such as the need for computational resources and the potential challenges in aligning the two modalities effectively.

## References

- Abdulaal, A.; Liu, Z.; and Lancewicki, T. 2021. Practical Approach to Asynchronous Multivariate Time Series Anomaly Detection and Localization. *KDD*.
- Bagnall, A.; Dau, H. A.; Lines, J.; Flynn, M.; Large, J.; Bostrom, A.; Southam, P.; and Keogh, E. 2018. The UEA multivariate time series classification archive, 2018. *arXiv preprint arXiv:1811.00075*.
- Belghazi, M. I.; Baratin, A.; Rajeswar, S.; Ozair, S.; Bengio, Y.; Courville, A.; and Hjelm, R. D. 2021. MINE: Mutual Information Neural Estimation. *arXiv:1801.04062*.
- Bell, A. J.; and Sejnowski, T. J. 1995. An information-maximization approach to blind separation and blind deconvolution. *Neural computation*, 7(6): 1129–1159.
- Brown, T.; Mann, B.; Ryder, N.; Subbiah, M.; Kaplan, J. D.; Dhariwal, P.; Neelakantan, A.; Shyam, P.; Sastry, G.; Askell, A.; et al. 2020. Language models are few-shot learners. *Advances in neural information processing systems*, 33: 1877–1901.
- Cao, D.; Jia, F.; Arik, S. O.; Pfister, T.; Zheng, Y.; Ye, W.; and Liu, Y. 2024. Tempo: Prompt-based generative pre-trained transformer for time series forecasting. *ICLR*.
- CDC. 2024. Illness. <https://gis.cdc.gov/grasp/fluview/fluportaldashboard.html>. Online; accessed 10 August 2024.
- Challu, C.; Olivares, K. G.; Oreshkin, B. N.; Ramirez, F. G.; Canseco, M. M.; and Dubrawski, A. 2023. Nhits: Neural hierarchical interpolation for time series forecasting. In *Proceedings of the AAAI Conference on Artificial Intelligence*.
- Chen, C.; Chen, X.; Ma, C.; Liu, Z.; and Liu, X. 2022. Gradient-based bi-level optimization for deep learning: A survey. *arXiv preprint arXiv:2207.11719*.
- Chen, C.; Oliveira, G. L.; Sharifi-Noghabi, H.; and Sylvain, T. 2024. Enhance Time Series Modeling by Integrating LLM. In *NeurIPS Workshop on Time Series in the Age of Large Models*.
- Chen, T.; and Guestrin, C. 2016. Xgboost: A scalable tree boosting system. In *Proceedings of the 22nd acm sigkdd international conference on knowledge discovery and data mining*, 785–794.
- Dempster, A.; Petitjean, F.; and Webb, G. I. 2020. ROCKET: exceptionally fast and accurate time series classification using random convolutional kernels. *Data Mining and Knowledge Discovery*, 34(5): 1454–1495.
- Devlin, J.; Chang, M.-W.; Lee, K.; and Toutanova, K. 2018. Bert: Pre-training of deep bidirectional transformers for language understanding. *arXiv preprint arXiv:1810.04805*.
- Fang, T.; Lu, N.; Niu, G.; and Sugiyama, M. 2024. Generalizing Importance Weighting to A Universal Solver for Distribution Shift Problems. *Proc. Adv. Neur. Inf. Proc. Syst (NeurIPS)*.
- Franceschi, J.-Y.; Dieuleveut, A.; and Jaggi, M. 2019. Un-supervised scalable representation learning for multivariate time series. *Advances in neural information processing systems*, 32.
- Freund, Y.; and Schapire, R. E. 1997. A decision-theoretic generalization of on-line learning and an application to boosting. *Journal of computer and system sciences*.
- Friedman, M. 1962. The interpolation of time series by related series. *Journal of the American Statistical Association*.
- Gao, J.; Song, X.; Wen, Q.; Wang, P.; Sun, L.; and Xu, H. 2020. Robusttad: Robust time series anomaly detection via decomposition and convolutional neural networks. *arXiv preprint arXiv:2002.09545*.
- Gruver, N.; Finzi, M.; Qiu, S.; and Wilson, A. G. 2024. Large language models are zero-shot time series forecasters. *Advances in Neural Information Processing Systems*, 36.
- Gruver, N.; Finzi, M. A.; Qiu, S.; and Wilson, A. G. 2023. Large Language Models Are Zero-Shot Time Series Forecasters. In *Thirty-seventh Conference on Neural Information Processing Systems*.
- Gu, A.; Goel, K.; and Ré, C. 2021. Efficiently modeling long sequences with structured state spaces. *arXiv preprint arXiv:2111.00396*.
- Hjelm, R. D.; Fedorov, A.; Lavoie-Marchildon, S.; Grewal, K.; Bachman, P.; Trischler, A.; and Bengio, Y. 2018. Learning deep representations by mutual information estimation and maximization. *arXiv preprint arXiv:1808.06670*.
- Hjelm, R. D.; Fedorov, A.; Lavoie-Marchildon, S.; Grewal, K.; Bachman, P.; Trischler, A.; and Bengio, Y. 2019. Learning deep representations by mutual information estimation and maximization. *arXiv:1808.06670*.
- Huang, Z.; Shi, X.; Zhang, C.; Wang, Q.; Cheung, K. C.; Qin, H.; Dai, J.; and Li, H. 2022. Flowformer: A transformer architecture for optical flow. In *European conference on computer vision*, 668–685. Springer.
- Hundman, K.; Constantinou, V.; Laporte, C.; Colwell, I.; and Söderström, T. 2018. Detecting Spacecraft Anomalies Using LSTMs and Nonparametric Dynamic Thresholding. *KDD*.
- Hyndman, R. J.; and Athanasopoulos, G. 2018. *Forecasting: principles and practice*. OTexts.
- Jiang, Y.; Pan, Z.; Zhang, X.; Garg, S.; Schneider, A.; Nevmyvaka, Y.; and Song, D. 2024. Empowering Time Series Analysis with Large Language Models: A Survey. *arXiv preprint arXiv:2402.03182*.
- Jin, M.; Wang, S.; Ma, L.; Chu, Z.; Zhang, J. Y.; Shi, X.; Chen, P.-Y.; Liang, Y.; Li, Y.-F.; Pan, S.; and Wen, Q. 2024. Time-LLM: Time Series Forecasting by Reprogramming Large Language Models. In *The Twelfth International Conference on Learning Representations*.
- Jin, M.; Wang, S.; Ma, L.; Chu, Z.; Zhang, J. Y.; Shi, X.; Chen, P.-Y.; Liang, Y.; Li, Y.-F.; Pan, S.; et al. 2023. Time-llm: Time series forecasting by reprogramming large language models. *arXiv preprint arXiv:2310.01728*.
- Kitaev, N.; Kaiser, L.; and Levskaya, A. 2020. Reformer: The Efficient Transformer. In *ICLR*.
- Lai, G.; Chang, W.-C.; Yang, Y.; and Liu, H. 2018. Modeling long-and short-term temporal patterns with deep neural networks. In *The 41st international ACM SIGIR conference on research & development in information retrieval*, 95–104.

- Lim, B.; and Zohren, S. 2021. Time-series forecasting with deep learning: a survey. *Philos. Trans. Royal Soc. A*.
- Linsker, R. 1988. Self-organization in a perceptual network. *Computer*, 21: 105–117.
- Liu, S.; Yu, H.; Liao, C.; Li, J.; Lin, W.; Liu, A. X.; and Dustdar, S. 2021. Pyraformer: Low-complexity pyramidal attention for long-range time series modeling and forecasting. In *ICLR*.
- Liu, Y.; Wu, H.; Wang, J.; and Long, M. 2022. Non-stationary transformers: Exploring the stationarity in time series forecasting. *Advances in Neural Information Processing Systems*, 35: 9881–9893.
- Mathur, A. P.; and Tippenhauer, N. O. 2016. SWaT: a water treatment testbed for research and training on ICS security. In *CySWATER*.
- Nie, Y.; Nguyen, N. H.; Sinthong, P.; and Kalagnanam, J. 2022. A time series is worth 64 words: Long-term forecasting with transformers. *arXiv preprint arXiv:2211.14730*.
- Nowozin, S.; Cseke, B.; and Tomioka, R. 2016. f-gan: Training generative neural samplers using variational divergence minimization. *Advances in neural information processing systems*, 29.
- Oreshkin, B. N.; Carпов, D.; Chapados, N.; and Bengio, Y. 2019. N-BEATS: Neural basis expansion analysis for interpretable time series forecasting. *ICLR*.
- PeMS. 2024. Traffic. <http://pems.dot.ca.gov/>. Online; accessed 10 August 2024.
- Radford, A.; Wu, J.; Child, R.; Luan, D.; Amodei, D.; Sutskever, I.; et al. 2019. Language models are unsupervised multitask learners. *OpenAI blog*.
- Ren, M.; Zeng, W.; Yang, B.; and Urtasun, R. 2018. Learning to reweight examples for robust deep learning. In *Proc. Int. Conf. Machine Lea. (ICML)*.
- Shu, J.; Xie, Q.; Yi, L.; Zhao, Q.; Zhou, S.; Xu, Z.; and Meng, D. 2019. Meta-weight-net: Learning an explicit mapping for sample weighting. *Proc. Adv. Neur. Inf. Proc. Syst (NeurIPS)*.
- Shwartz-Ziv, R.; and Tishby, N. 2017. Opening the Black Box of Deep Neural Networks via Information. *arXiv:1703.00810*.
- Spyros Makridakis. 2018. M4 dataset.
- Su, Y.; Zhao, Y.; Niu, C.; Liu, R.; Sun, W.; and Pei, D. 2019. Robust Anomaly Detection for Multivariate Time Series through Stochastic Recurrent Neural Network. *KDD*.
- Sun, C.; Li, Y.; Li, H.; and Hong, S. 2023. TEST: Text prototype aligned embedding to activate LLM’s ability for time series. *arXiv preprint arXiv:2308.08241*.
- Sun, F.-Y.; Hoffmann, J.; Verma, V.; and Tang, J. 2019. Infograph: Unsupervised and semi-supervised graph-level representation learning via mutual information maximization. *arXiv preprint arXiv:1908.01000*.
- Sun, Y.; Kamel, M. S.; Wong, A. K.; and Wang, Y. 2007. Cost-sensitive boosting for classification of imbalanced data. *Pattern recognition*.
- Sylvain, T.; Petrini, L.; and Hjelm, D. 2019. Locality and Compositionality in Zero-Shot Learning. In *International Conference on Learning Representations*.
- Tishby, N.; Pereira, F. C.; and Bialek, W. 2000. The information bottleneck method. *arXiv:physics/0004057*.
- Touvron, H.; Martin, L.; Stone, K.; Albert, P.; Almahairi, A.; Babaei, Y.; Bashlykov, N.; Batra, S.; Bhargava, P.; Bhosale, S.; et al. 2023. Llama 2: Open foundation and fine-tuned chat models. *arXiv preprint arXiv:2307.09288*.
- UCI. 2015. Electricity. <https://archive.ics.uci.edu/ml/datasets/ElectricityLoadDiagrams20112014>. Online; accessed 10 August 2024.
- Wang, S.; Wu, H.; Shi, X.; Hu, T.; Luo, H.; Ma, L.; Zhang, J. Y.; and ZHOU, J. 2023. TimeMixer: Decomposable Multi-scale Mixing for Time Series Forecasting. In *ICLR*.
- Wang, Z.; Xu, Q.; Yang, Z.; He, Y.; Cao, X.; and Huang, Q. 2024. A Unified Generalization Analysis of Re-Weighting and Logit-Adjustment for Imbalanced Learning. *Proc. Adv. Neur. Inf. Proc. Syst (NeurIPS)*.
- Wen, Q.; Yang, L.; Zhou, T.; and Sun, L. 2022. Robust time series analysis and applications: An industrial perspective. In *KDD*.
- Wetterstation. 2024. Weather. <https://www.bgc-jena.mpg.de/wetter/>. Online; accessed 10 August 2024.
- Woo, G.; Liu, C.; Sahoo, D.; Kumar, A.; and Hoi, S. C. H. 2022. ETSformer: Exponential Smoothing Transformers for Time-series Forecasting. *arXiv preprint arXiv:2202.01381*.
- Wu, H.; Hu, T.; Liu, Y.; Zhou, H.; Wang, J.; and Long, M. 2023. TimesNet: Temporal 2D-Variation Modeling for General Time Series Analysis. In *The Eleventh International Conference on Learning Representations*.
- Wu, H.; Xu, J.; Wang, J.; and Long, M. 2021. Autoformer: Decomposition Transformers with Auto-Correlation for Long-Term Series Forecasting. In *NeurIPS*.
- Xu, J.; Wu, H.; Wang, J.; and Long, M. 2021. Anomaly Transformer: Time Series Anomaly Detection with Association Discrepancy. In *ICLR*.
- Xue, H.; and Salim, F. D. 2023. Promptcast: A new prompt-based learning paradigm for time series forecasting. *IEEE Transactions on Knowledge and Data Engineering*.
- Yi, K.; Zhang, Q.; Fan, W.; Wang, S.; Wang, P.; He, H.; An, N.; Lian, D.; Cao, L.; and Niu, Z. 2024. Frequency-domain MLPs are more effective learners in time series forecasting. *Proc. Adv. Neur. Inf. Proc. Syst (NeurIPS)*.
- Yuan, H.; Dou, H.; Jiang, X.; and Deng, Y. 2024a. Task-aware world model learning with meta weighting via bi-level optimization. *Proc. Adv. Neur. Inf. Proc. Syst (NeurIPS)*.
- Yuan, Y.; Chen, C. S.; Liu, Z.; Neiswanger, W.; and Liu, X. S. 2024b. Importance-aware co-teaching for offline model-based optimization. *Advances in Neural Information Processing Systems*.
- Zeng, A.; Chen, M.; Zhang, L.; and Xu, Q. 2023. Are transformers effective for time series forecasting? In *Proceedings of the AAAI conference on artificial intelligence*.
- Zhang, T.; Zhang, Y.; Cao, W.; Bian, J.; Yi, X.; Zheng, S.; and Li, J. 2022. Less is more: Fast multivariate time series forecasting with light sampling-oriented mlp structures. *arXiv preprint arXiv:2207.01186*.

Zhang, X.; Chen, J.; Wang, H.; Xie, H.; Liu, Y.; Lui, J.; and Li, H. 2024. Uncertainty-aware instance reweighting for off-policy learning. *Proc. Adv. Neur. Inf. Proc. Syst (NeurIPS)*.

Zhou, H.; Hu, C.; Yuan, Y.; Cui, Y.; Jin, Y.; Chen, C.; Wu, H.; Yuan, D.; Jiang, L.; Wu, D.; et al. 2024a. Large language model (llm) for telecommunications: A comprehensive survey on principles, key techniques, and opportunities. *arXiv preprint arXiv:2405.10825*.

Zhou, H.; Zhang, S.; Peng, J.; Zhang, S.; Li, J.; Xiong, H.; and Zhang, W. 2021a. Informer: Beyond efficient transformer for long sequence time-series forecasting. In *Proceedings of the AAAI conference on artificial intelligence*.

Zhou, H.; Zhang, S.; Peng, J.; Zhang, S.; Li, J.; Xiong, H.; and Zhang, W. 2021b. Informer: Beyond Efficient Transformer for Long Sequence Time-Series Forecasting. In *AAAI*.

Zhou, T.; Ma, Z.; Wen, Q.; Wang, X.; Sun, L.; and Jin, R. 2022. FEDformer: Frequency enhanced decomposed transformer for long-term series forecasting. In *ICML*.

Zhou, T.; Niu, P.; Sun, L.; Jin, R.; et al. 2024b. One fits all: Power general time series analysis by pretrained lm. *Advances in neural information processing systems*, 36.

## A Reproducibility Checklist

This paper:

- Includes a conceptual outline and/or pseudocode description of AI methods introduced (yes/partial/no/NA) YES
- Clearly delineates statements that are opinions, hypothesis, and speculation from objective facts and results (yes/no) YES
- Provides well marked pedagogical references for less-familare readers to gain background necessary to replicate the paper (yes/no) YES

Does this paper make theoretical contributions? (yes/no) NO

Does this paper rely on one or more datasets? (yes/no) YES

If yes, please complete the list below.

- A motivation is given for why the experiments are conducted on the selected datasets (yes/partial/no/NA) YES
- All novel datasets introduced in this paper are included in a data appendix. (yes/partial/no/NA) NA
- All novel datasets introduced in this paper will be made publicly available upon publication of the paper with a license that allows free usage for research purposes. (yes/partial/no/NA) NA
- All datasets drawn from the existing literature (potentially including authors' own previously published work) are accompanied by appropriate citations. (yes/no/NA) YES
- All datasets drawn from the existing literature (potentially including authors' own previously published work) are publicly available. (yes/partial/no/NA) YES
- All datasets that are not publicly available are described in detail, with explanation why publicly available alternatives are not scientifically satisfying. (yes/partial/no/NA) NA

Does this paper include computational experiments? (yes/no) YES

If yes, please complete the list below.

- Any code required for pre-processing data is included in the appendix. (yes/partial/no) YES. The code is available at [https://anonymous.4open.science/r/llm\\_ts\\_anonymous-F07D/README.MD](https://anonymous.4open.science/r/llm_ts_anonymous-F07D/README.MD)
- All source code required for conducting and analyzing the experiments is included in a code appendix. (yes/partial/no) YES
- All source code required for conducting and analyzing the experiments will be made publicly available upon publication of the paper with a license that allows free usage for research purposes. (yes/partial/no) YES
- All source code implementing new methods have comments detailing the implementation, with references to the paper where each step comes from (yes/partial/no) YES
- If an algorithm depends on randomness, then the method used for setting seeds is described in a way sufficient to allow replication of results. (yes/partial/no/NA) YES
- This paper specifies the computing infrastructure used for running experiments (hardware and software), including GPU/CPU models; amount of memory; operating system; names and versions of relevant software libraries and frameworks. (yes/partial/no) YES
- This paper formally describes evaluation metrics used and explains the motivation for choosing these metrics. (yes/partial/no) YES
- This paper states the number of algorithm runs used to compute each reported result. (yes/no) YES
- Analysis of experiments goes beyond single-dimensional summaries of performance (e.g., average; median) to include measures of variation, confidence, or other distributional information. (yes/no) YES
- The significance of any improvement or decrease in performance is judged using appropriate statistical tests (e.g., Wilcoxon signed-rank). (yes/partial/no) NA
- This paper lists all final (hyper-)parameters used for each model/algorithm in the paper's experiments. (yes/partial/no/NA) YES
- This paper states the number and range of values tried per (hyper-) parameter during development of the paper, along with the criterion used for selecting the final parameter setting. (yes/partial/no/NA) YES

## B Appendix

### B.1 Mutual Information Recalculation

Recall that mutual information can be calculated using the equation:

$$I(\theta, \beta) = \mathbb{E}_{\mathbb{S}}[-sp(-T_{\beta}(\mathbf{h}_{\theta}^m(\mathbf{x}), \mathbf{h}^l(\mathbf{t}))) - \mathbb{E}_{\mathbb{S} \times \tilde{\mathbb{S}}} [sp(T_{\beta}(\mathbf{h}_{\theta}^m(\mathbf{x}), \mathbf{h}^l(\tilde{\mathbf{t}})))] , \quad (8)$$

where  $T_{\beta}$  signifies the discriminator characterized by parameters  $\beta$ , and  $sp$  denotes the softplus function. Notably,  $(\mathbf{x}, \mathbf{t})$  symbolizes a sample from the dataset  $\mathbb{S}$ , while  $(\tilde{\mathbf{x}}, \tilde{\mathbf{t}})$  represents a different sample from the dataset  $\tilde{\mathbb{S}} = \mathbb{S}$ .

This formulation presumes a uniform distribution of samples. However, we have already computed probabilities  $p_I^i$  for each sample, which introduces a non-uniform distribution. For a batch of  $N$  samples, the expected value is computed as

$$\mathbb{E}_{\mathbb{S}}[-sp(-T_{\beta}(\mathbf{h}_{\theta}^m(\mathbf{x}), \mathbf{h}^l(\mathbf{t}))) = - \sum_{i=1}^N p_I^i sp(-T_{\beta}(\mathbf{h}_{\theta}^m(\mathbf{x}^i), \mathbf{h}^l(\mathbf{t}^i))). \quad (9)$$

$$\mathbb{E}_{\mathbb{S} \times \tilde{\mathbb{S}}} [sp(T_{\beta}(\mathbf{h}_{\theta}^m(\mathbf{x}), \mathbf{h}^l(\tilde{\mathbf{t}})))] = \sum_i \sum_{i \neq j} \hat{p}^{ij} sp(T_{\beta}(\mathbf{h}_{\theta}^m(\mathbf{x}^i), \mathbf{h}^l(\tilde{\mathbf{t}}^j))). \quad (10)$$

Here,  $\hat{p}^{ij}$  is defined as  $\frac{p_I^i \cdot p_I^j}{\sum_i \sum_{i \neq j} p_I^i \cdot p_I^j}$ , adjusting for the non-uniform distribution of sample probabilities. As  $p_I^i$  is produced from the weighting network  $\alpha$ , we can also write  $I(\theta, \beta)$  as  $I(\theta, \beta, \alpha)$ .

### B.2 Experimental Settings

following (Shu et al. 2019), the weighting network comprises a two-layer MLP with a hidden size of 100, and we set the learning rate  $\eta_2$  for this network at 0.001. The learning rate  $\eta_0$  of the discriminator is set as 0.001 at the first epoch and then decreases to 0.0001 for the rest of epochs.

### B.3 Standard Deviation Results

Table 8 presents the results along with standard deviations to underscore the consistency and reliability of our method’s performance.

### B.4 Showcases

To provide a clear comparison among different models, we showcase the forecasting task results on ETTh1 (96-96) and ETTm1 (96-336) using three models: *LLM-TS*, TimesNet, and GPT4TS. As shown in Figures 5 and 6, our LLM-TS model produces significantly more accurate predictions, demonstrating its effectiveness.

To illustrate the performance improvements achieved by the LLM-TS Integrator framework, we introduce a case study. We created a training set with a weighted sine function:

$$\sum_{i=1}^4 \omega_i \sin(f_i t + p_i) + \epsilon N(0, 1) \quad (11)$$

where  $w_1 = 0.1$ ,  $w_2 = 0.2$ ,  $w_3 = 0.3$ ,  $w_4 = 0.4$ ;  $f_1 = \frac{1}{40}$ ,  $f_2 = \frac{1}{45}$ ,  $f_3 = \frac{1}{50}$ ,  $f_4 = \frac{1}{55}$ ;  $p_1 = 0$ ,  $p_2 = 1$ ,  $p_3 = 2$ ,  $p_4 = 3$ ; and  $\epsilon = 0.1$  is the noise level. We generated a long sequence of length 10,000 and then sampled a batch of size 64 with a sequence length of 96 and a prediction length of 336 to train GPT4TS, TimesNet, and LLM-TS on this data for 1,000 iterations. For testing, we created a test set with frequency  $f = \frac{1}{20}$ , which is greater than  $\max(f_1, f_2, f_3, f_4)$ , and used  $p = 2.5$ ,  $w = 1$  and  $\epsilon = 0.1$ .

As shown in Figure 7, Figure 8 and Figure 9, we can know:

- GPT4TS fails to accurately capture periodic information as it relies solely on a language model without incorporating traditional mathematical modelling.
- TimesNet generally captures periodic information due to the use of the FFT mathematical operator, but it still does not perfectly match the ground truth.
- LLM-TS captures periodic information and better matches the ground truth by integrating rich language model insights into the traditional TimesNet model.

This case study highlights how the LLM-TS Integrator framework benefits from both inherent properties of traditional TS models and pattern recognition abilities of LLMs, demonstrating the effectiveness of our approach.

### B.5 Template Variation

We conducted additional experiments on the ETTh1 dataset for long-term forecasting with GPT2. The original template achieves a Mean Squared Error (MSE) of 0.464 and a Mean Absolute Error (MAE) of 0.458. We tested variations of the template by changing the original context from "The Electricity Transformer Temperature is a crucial indicator in electric power long-term deployment." to:

- Variation 1: "The temperature of the electricity transformer is a vital metric for long-term electric power deployment."
- Variation 2: "Monitoring the temperature of electricity transformers is essential for the long-term deployment of electric power."
- Variation 3: "The temperature of electricity transformers serves as a key indicator in the long-term deployment of electric power."
- Variation 4: No template.

Besides, we also consider the following changes:

- w/o Input Statistics: excluding input statistical data from our analysis.
- w/o Mean, Max, Median: remove mean, max and median informatino.
- w/o Lags: remove lags information.

The performance of these variations is summarized in Table 9. These results indicate that the performance is quite similar across different variations, supporting the robustness of our approach regardless of minor template modifications. For further details on the template implementation, refer to our code repository at [https://anonymous.4open.science/r/llm\\_ts\\_anonymous-F07D/utis/tools.py](https://anonymous.4open.science/r/llm_ts_anonymous-F07D/utis/tools.py).

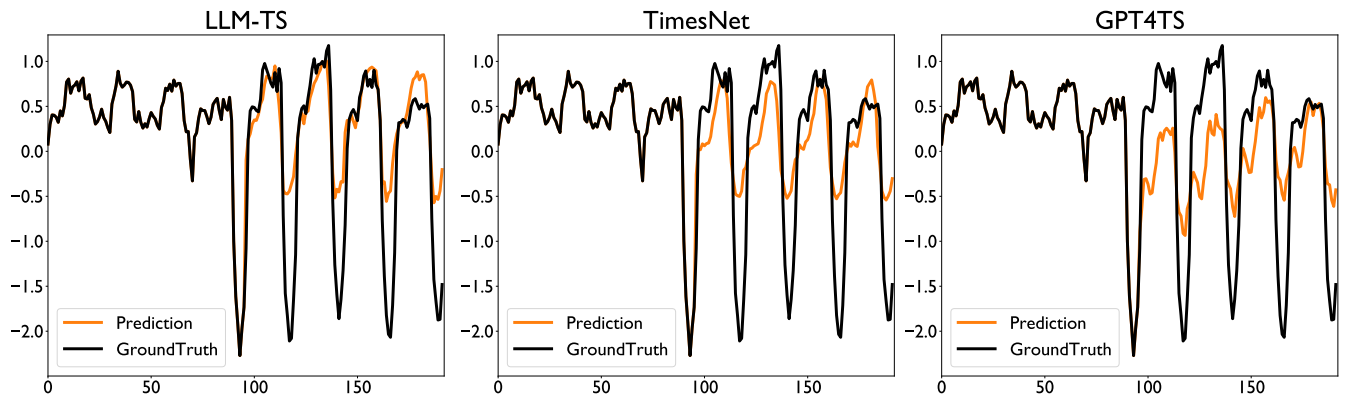


Figure 5: ETTh1

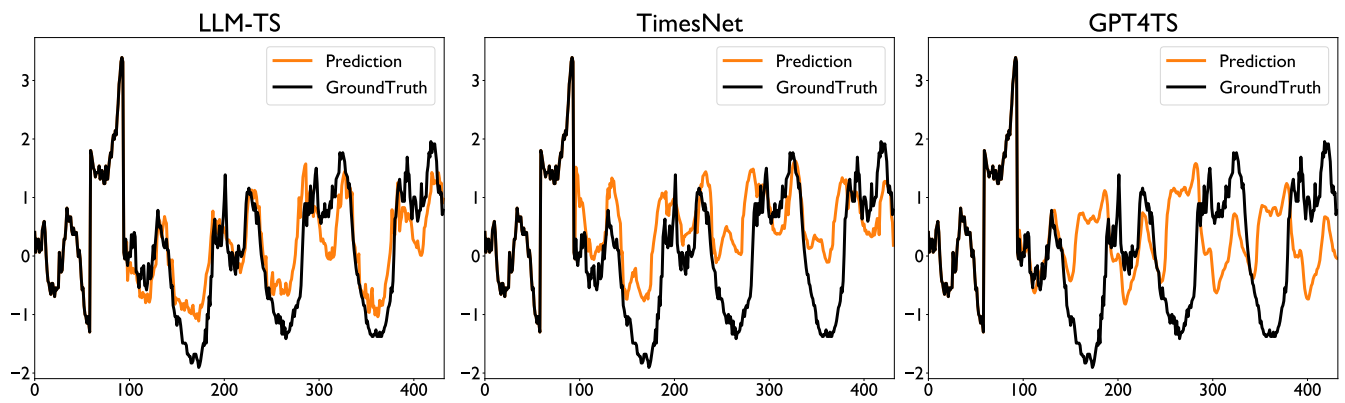


Figure 6: ETTm1

Table 8: Ablation results with standard deviation.

Methods	Ours		w/o mutual		w/o reweight		TimesNet		
Metric	MSE	MAE	MSE	MAE	MSE	MAE	MSE	MAE	
<i>Weather</i>	96	0.166 ± 0.002	0.217 ± 0.002	0.168 ± 0.003	0.218 ± 0.005	0.181 ± 0.003	0.232 ± 0.001	0.174 ± 0.003	0.224 ± 0.002
	192	0.229 ± 0.003	0.269 ± 0.003	0.227 ± 0.004	0.268 ± 0.003	0.230 ± 0.002	0.270 ± 0.004	0.235 ± 0.001	0.272 ± 0.003
	336	0.278 ± 0.002	0.302 ± 0.003	0.298 ± 0.004	0.318 ± 0.003	0.283 ± 0.004	0.306 ± 0.002	0.285 ± 0.002	0.307 ± 0.002
	720	0.354 ± 0.001	0.351 ± 0.001	0.361 ± 0.002	0.356 ± 0.001	0.361 ± 0.002	0.355 ± 0.001	0.365 ± 0.001	0.358 ± 0.000
<i>ETTh1</i>	96	0.403 ± 0.005	0.420 ± 0.003	0.402 ± 0.004	0.422 ± 0.002	0.408 ± 0.003	0.428 ± 0.002	0.414 ± 0.006	0.431 ± 0.004
	192	0.440 ± 0.009	0.441 ± 0.004	0.459 ± 0.006	0.455 ± 0.005	0.469 ± 0.005	0.460 ± 0.003	0.463 ± 0.010	0.456 ± 0.006
	336	0.471 ± 0.006	0.457 ± 0.004	0.471 ± 0.005	0.457 ± 0.004	0.492 ± 0.004	0.474 ± 0.004	0.487 ± 0.007	0.466 ± 0.005
	720	0.503 ± 0.005	0.487 ± 0.004	0.535 ± 0.003	0.507 ± 0.003	0.485 ± 0.006	0.478 ± 0.007	0.517 ± 0.004	0.494 ± 0.004
<i>ETTm1</i>	96	0.329 ± 0.014	0.371 ± 0.006	0.341 ± 0.010	0.377 ± 0.008	0.350 ± 0.011	0.387 ± 0.005	0.340 ± 0.011	0.377 ± 0.007
	192	0.380 ± 0.009	0.398 ± 0.004	0.404 ± 0.010	0.413 ± 0.005	0.383 ± 0.010	0.397 ± 0.005	0.406 ± 0.012	0.408 ± 0.004
	336	0.418 ± 0.004	0.425 ± 0.004	0.432 ± 0.005	0.428 ± 0.002	0.410 ± 0.004	0.411 ± 0.003	0.424 ± 0.006	0.425 ± 0.003
	720	0.476 ± 0.008	0.440 ± 0.005	0.468 ± 0.009	0.449 ± 0.004	0.467 ± 0.007	0.448 ± 0.003	0.485 ± 0.010	0.461 ± 0.006
<i>LLI</i>	24	1.921 ± 0.201	0.898 ± 0.033	2.170 ± 0.174	0.947 ± 0.039	1.934 ± 0.170	0.925 ± 0.034	2.072 ± 0.211	0.948 ± 0.026
	36	2.151 ± 0.061	0.933 ± 0.035	2.093 ± 0.119	0.889 ± 0.041	2.505 ± 0.179	1.020 ± 0.017	2.494 ± 0.125	1.019 ± 0.007
	48	2.062 ± 0.090	0.892 ± 0.019	2.418 ± 0.058	0.959 ± 0.014	2.325 ± 0.201	0.948 ± 0.062	2.298 ± 0.066	0.964 ± 0.011
	60	1.759 ± 0.214	0.853 ± 0.061	2.203 ± 0.181	0.971 ± 0.048	1.926 ± 0.152	0.896 ± 0.039	2.198 ± 0.070	0.963 ± 0.017

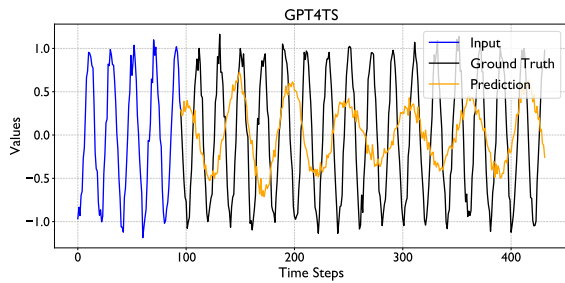


Figure 7: GPT4TS on synthetic data

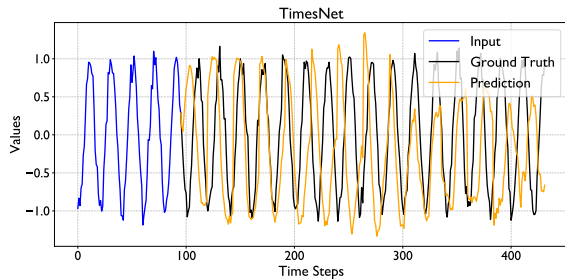


Figure 8: TimesNet on synthetic data

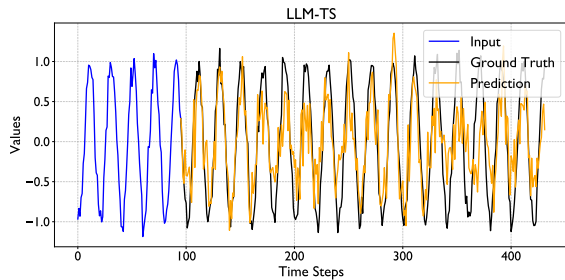


Figure 9: LLM-TS on synthetic data

Table 9: Performance across different template variations

Template Variation	MSE	MAE
Original Template	0.464 ± 0.004	0.458 ± 0.005
Variation 1	0.460 ± 0.005	0.456 ± 0.003
Variation 2	0.465 ± 0.006	0.460 ± 0.005
Variation 3	0.464 ± 0.004	0.459 ± 0.003
Variation 4 (No template)	0.466 ± 0.005	0.460 ± 0.005
w/o Input Statistics	0.468 ± 0.004	0.462 ± 0.004
w/o Mean/Max/Median	0.465 ± 0.004	0.459 ± 0.003
w/o Lags	0.467 ± 0.003	0.460 ± 0.005

## B.6 Model Efficiency Analysis

Compared to TimesNet, our *LLM-TS integrator* introduces additional costs due to the mutual information and sample weighting modules. However, after training, the inference cost of our method is the same as TimesNet. We detail the time cost of each component for ETTh1 and ETTm1 tasks, using a batch size of 32 on a 32G V100 GPU. As shown in Table 10, the training cost of our method is reasonable, given that it achieves the best performance across most tasks.

It is important to note that we use the pre-trained LLM to obtain the text embeddings only once. These embeddings can then be used throughout the training process. For instance, obtaining the embeddings for the ETTh1 dataset using the llama-3b model on an A100 GPU takes approximately 1 hour. After this, the embeddings are utilized in our framework to train the model, and in the final output of the TimesNet model. This ensures that the inference time of our method is identical to that of the TimesNet model.

As detailed in the TimesNet paper, our backbone model TimesNet is relatively small with 0.067 MB parameters. For comparison, other models have the following sizes: Non-stationary Transformer has 1.884 MB, Autoformer has 1.848 MB, FEDformer has 2.9 MB, LightTS has 0.163 MB, DLinear has 0.296 MB, ETSformer has 1.123 MB, Informer has 1.903 MB, Reformer has 1.157 MB, and Pyraformer has 1.308 MB. The introduced mutual information network con-

sists of only two linear layers of size  $64 \times 64$  and  $64 \times 4096$ , which is negligible in terms of additional parameters. Similarly, the introduced MLP network consists of four layers:  $1 \times 100$ ,  $100 \times 1$ ,  $1 \times 1$ , and  $1 \times 1$ , and the number of parameters is also negligible.

Thus, our model remains very small and efficient, with inference time identical to TimesNet (as the mutual information component is only used during training). Given that many TS models are primarily used for inference, our approach offers effective performance gains with minimal additional computational cost.

### B.7 Full Results of Short-term Forecasting

Table 11 displays the comprehensive results for short-term forecasting.

### B.8 Full Results of Long-Term Forecasting

Full results for long-term forecasting are presented in Table 12.

### B.9 Full Results of Imputation.

Table 13 contains the detailed results of our imputation tasks.

### B.10 Full Results of Classification

Table 14 contains the comprehensive results for classification.

### B.11 Full Results of Anomaly Detection

Full results for anomaly detection are detailed in Table 15.

### B.12 Further Ablation Studies

**Mutual Information Estimator.** In the main paper, we utilize the Jensen-Shannon mutual information (MI) estimator. Additionally, we explore the Mutual Information Neural Estimator (MINE) (Hjelm et al. 2018). We evaluate both estimators on two tasks, ETTh1 and ETTm1, with results averaged over four prediction lengths. For ETTh1, the MSE and MAE using the original Jensen-Shannon estimator are 0.454 and 0.451, respectively, compared to 0.460 and 0.457 with MINE. For ETTm1, the MSE and MAE are 0.401 and 0.409 with the original estimator, and 0.402 and 0.410 with MINE. These comparisons highlight the robustness of our method across different mutual information estimators.

**Sample Reweighting Illustration.** Figures 11, 10, 12, and 13 display the learned weighting network applied to various datasets: MSL for anomaly detection, Weather for forecasting, ETTh1 for imputation, and PEMS-SF for classification. These visualizations corroborate our hypothesis: the sample weight  $\omega_O$  increases with the prediction loss  $l_O$ , while the weight  $\omega_I$  decreases as  $l_O$  increases. This observed pattern supports the efficacy of our reweighting strategy.

**Static Weighting Scheme.** We also explore a static weighting scheme as a contrast to the dynamic weighting used in our sample reweighting module. This scheme balances the prediction loss and mutual information loss, with a ratio of 0.0 representing pure prediction loss and 1.0 representing pure mutual information loss. As shown in Table 18, the

static approach underperforms relative to our dynamic sample weighting module, demonstrating the superior effectiveness of our method.

**Comprehensive Results.** The detailed performance of various traditional TS models and LLMs is presented in Table 16 and Table 17.

Table 10: Cost Comparison per step(s).

Methods	Overall	TimesNet	Mutual Information	Sample Reweighting
ETTh1	3.177	0.126	0.577	2.474
Weather	5.563	0.436	1.094	4.033

Table 11: Full results of short-term forecasting.

Methods	LLM-TS	TimesNet	GPT4TS	TIME-LLM	PatchTST	N-HiTS	N-BEATS	FEDformer	Stationary	Autoformer
Yearly	<i>SMAPE</i>	13.369	13.512	13.531	13.419	13.477	13.418	13.436	13.728	13.974
	<i>MASE</i>	3.021	3.065	3.015	3.0050	3.019	3.045	3.043	3.048	3.134
	<i>OWA</i>	0.789	0.799	0.793	0.789	0.792	0.793	0.794	0.803	0.807
Quarterly	<i>SMAPE</i>	10.020	10.069	10.177	10.110	10.38	10.202	10.124	10.792	10.958
	<i>MASE</i>	1.162	1.178	1.194	1.178	1.233	1.194	1.169	1.283	1.325
	<i>OWA</i>	0.878	0.887	0.898	0.889	0.921	0.899	0.886	0.958	0.981
Monthly	<i>SMAPE</i>	12.696	12.783	12.894	12.980	12.959	12.791	12.677	14.260	13.917
	<i>MASE</i>	0.936	0.949	0.956	0.963	0.970	0.969	0.937	1.102	1.097
	<i>OWA</i>	0.880	0.889	0.897	0.903	0.905	0.899	0.880	1.012	0.998
Others	<i>SMAPE</i>	4.916	4.954	4.940	4.795	4.952	5.061	4.925	4.954	6.302
	<i>MASE</i>	3.310	3.364	3.228	3.178	3.347	3.216	3.391	3.264	4.064
	<i>OWA</i>	1.039	1.052	1.029	1.006	1.049	1.040	1.053	1.036	1.304
Average	<i>SMAPE</i>	11.819	11.908	11.991	11.983	12.059	11.927	11.851	12.840	12.780
	<i>MASE</i>	1.588	1.612	1.600	1.595	1.623	1.613	1.599	1.701	1.771
	<i>OWA</i>	0.851	0.860	0.861	0.859	0.869	0.861	0.855	0.918	0.930

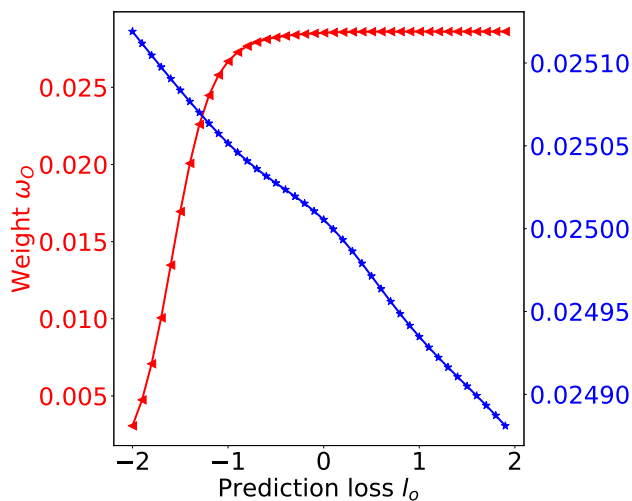


Figure 10: Forecasting.

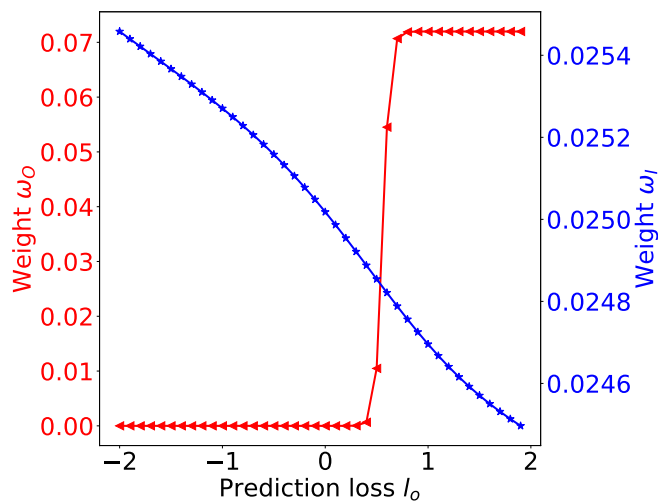


Figure 11: Anomaly detection

Table 12: Full results for long-term forecasting. We use prediction length  $O \in \{96, 192, 336, 720\}$  except for ILI and  $O \in \{24, 36, 48, 60\}$  for ILI. A lower MSE indicates better performance.

Methods	LLM-TS		TimesNet		TIME-LLM		DLinear		PatchTST		GPT4TS		FEDformer		TEST		Stationary		ETSformer		
Metric	MSE	MAE	MSE	MAE	MSE	MAE	MSE	MAE	MSE	MAE	MSE	MAE	MSE	MAE	MSE	MAE	MSE	MAE	MSE	MAE	
<i>Weather</i>	96	0.166	0.217	0.174	0.224	0.202	0.239	0.196	0.255	0.186	0.227	0.196	0.234	0.217	0.296	0.214	0.264	0.173	0.223	0.197	0.281
	192	0.229	0.269	0.235	0.272	0.245	0.277	0.237	0.296	0.234	0.265	0.241	0.271	0.276	0.336	0.262	0.298	0.245	0.285	0.237	0.312
	336	0.278	0.302	0.235	0.272	0.300	0.313	0.283	0.335	0.284	0.301	0.296	0.308	0.339	0.380	0.310	0.329	0.321	0.338	0.298	0.353
	720	0.354	0.351	0.365	0.358	0.369	0.356	0.345	0.381	0.356	0.349	0.367	0.354	0.403	0.428	0.378	0.370	0.414	0.410	0.352	0.288
	<i>Avg</i>	0.257	0.285	0.265	0.290	0.279	0.296	0.265	0.317	0.265	0.285	0.275	0.292	0.309	0.360	0.291	0.315	0.288	0.314	0.271	0.334
<i>ETTh1</i>	96	0.403	0.420	0.414	0.431	0.414	0.422	0.386	0.400	0.460	0.447	0.409	0.415	0.376	0.419	0.411	0.426	0.513	0.491	0.494	0.479
	192	0.440	0.441	0.463	0.456	0.466	0.450	0.437	0.432	0.512	0.477	0.468	0.446	0.420	0.448	0.475	0.461	0.534	0.504	0.538	0.504
	336	0.471	0.457	0.487	0.466	0.515	0.475	0.481	0.459	0.546	0.496	0.503	0.461	0.459	0.465	0.508	0.482	0.588	0.535	0.574	0.521
	720	0.503	0.487	0.517	0.494	0.503	0.487	0.519	0.516	0.544	0.517	0.510	0.482	0.506	0.507	0.504	0.494	0.643	0.616	0.562	0.535
	<i>Avg</i>	0.454	0.451	0.470	0.462	0.474	0.459	0.456	0.452	0.516	0.484	0.473	0.451	0.440	0.460	0.475	0.466	0.570	0.537	0.542	0.510
<i>ETTh2</i>	96	0.322	0.366	0.340	0.374	0.306	0.353	0.333	0.387	0.308	0.355	0.298	0.350	0.358	0.397	0.328	0.374	0.476	0.458	0.340	0.391
	192	0.400	0.409	0.399	0.410	0.386	0.399	0.477	0.476	0.393	0.405	0.376	0.399	0.429	0.439	0.403	0.418	0.512	0.493	0.430	0.439
	336	0.432	0.435	0.452	0.452	0.460	0.458	0.594	0.541	0.427	0.436	0.430	0.439	0.496	0.487	0.455	0.458	0.552	0.551	0.485	0.479
	720	0.430	0.442	0.462	0.468	0.442	0.451	0.831	0.657	0.436	0.450	0.428	0.451	0.463	0.474	0.470	0.477	0.562	0.560	0.500	0.497
	<i>Avg</i>	0.396	0.413	0.413	0.426	0.398	0.415	0.559	0.515	0.391	0.411	0.383	0.410	0.437	0.449	0.414	0.432	0.526	0.516	0.439	0.452
<i>ETTm1</i>	96	0.329	0.371	0.340	0.377	0.393	0.398	0.345	0.372	0.352	0.374	0.350	0.369	0.379	0.419	0.336	0.373	0.386	0.398	0.375	0.398
	192	0.380	0.398	0.406	0.408	0.412	0.405	0.380	0.389	0.390	0.393	0.387	0.387	0.426	0.441	0.381	0.399	0.459	0.444	0.408	0.410
	336	0.418	0.425	0.424	0.425	0.442	0.425	0.413	0.413	0.418	0.414	0.418	0.407	0.445	0.459	0.411	0.418	0.495	0.464	0.435	0.428
	720	0.476	0.440	0.485	0.461	0.502	0.457	0.474	0.453	0.462	0.449	0.477	0.437	0.543	0.490	0.478	0.454	0.585	0.516	0.499	0.462
	<i>Avg</i>	0.401	0.409	0.414	0.418	0.437	0.421	0.403	0.407	0.406	0.407	0.408	0.400	0.448	0.452	0.402	0.411	0.481	0.456	0.429	0.425
<i>ETTm2</i>	96	0.189	0.266	0.185	0.264	0.193	0.281	0.193	0.292	0.183	0.270	0.185	0.271	0.203	0.287	0.230	0.307	0.192	0.274	0.189	0.280
	192	0.253	0.307	0.252	0.306	0.254	0.315	0.284	0.363	0.255	0.314	0.250	0.312	0.269	0.328	0.284	0.338	0.280	0.339	0.253	0.319
	336	0.315	0.345	0.323	0.350	0.320	0.355	0.369	0.427	0.309	0.347	0.314	0.351	0.325	0.366	0.340	0.370	0.334	0.361	0.314	0.357
	720	0.421	0.408	0.415	0.403	0.426	0.416	0.554	0.522	0.412	0.404	0.410	0.408	0.421	0.415	0.436	0.420	0.417	0.413	0.414	0.413
	<i>Avg</i>	0.295	0.331	0.294	0.331	0.298	0.342	0.350	0.401	0.290	0.334	0.290	0.335	0.305	0.349	0.323	0.359	0.306	0.347	0.293	0.342
<i>ILI</i>	24	1.921	0.898	2.072	0.948	2.589	1.054	2.398	1.040	2.229	0.894	5.259	1.689	3.228	1.260	3.371	1.231	2.294	0.945	2.527	1.020
	36	2.151	0.933	2.494	1.019	2.996	1.194	2.646	1.088	2.330	0.925	6.136	1.831	2.679	1.080	3.725	1.322	1.825	0.848	2.615	1.007
	48	2.062	0.892	2.298	0.964	2.714	1.095	2.614	1.086	2.140	0.894	4.670	1.562	2.622	1.078	3.291	1.237	2.010	0.900	2.359	0.972
	60	1.759	0.853	2.198	0.963	2.605	1.050	2.804	1.146	2.037	0.912	4.402	1.517	2.857	1.157	2.907	1.136	2.178	0.963	2.487	1.016
	<i>Avg</i>	1.973	0.894	2.266	0.974	2.726	1.098	2.616	1.090	2.184	0.906	5.117	1.650	2.847	1.144	3.324	1.232	2.077	0.914	2.497	1.004
<i>ECL</i>	96	0.167	0.271	0.169	0.273	0.207	0.292	0.197	0.282	0.190	0.296	0.186	0.273	0.193	0.308	0.218	0.309	0.169	0.273	0.187	0.304
	192	0.178	0.280	0.186	0.288	0.209	0.297	0.196	0.285	0.199	0.304	0.190	0.278	0.201	0.315	0.220	0.311	0.182	0.286	0.199	0.315
	336	0.198	0.302	0.206	0.305	0.224	0.312	0.209	0.301	0.217	0.319	0.204	0.291	0.214	0.329	0.234	0.323	0.200	0.304	0.212	0.329
	720	0.233	0.344	0.231	0.327	0.277	0.359	0.245	0.333	0.258	0.352	0.245	0.297	0.325	0.355	0.276	0.354	0.222	0.321	0.233	0.345
	<i>Avg</i>	0.194	0.299	0.198	0.298	0.229	0.315	0.212	0.300	0.216	0.318	0.206	0.285	0.214	0.327	0.237	0.324	0.193	0.296	0.208	0.323
<i>Traffic</i>	96	0.587	0.315	0.589	0.313	0.609	0.402	0.650	0.396	0.526	0.347	0.563	0.378	0.587	0.366	0.589	0.390	0.612	0.338	0.607	0.392
	192	0.612	0.326	0.627	0.337	0.586	0.382	0.598	0.370	0.522	0.332	0.549	0.367	0.604	0.373	0.567	0.380	0.613	0.340	0.621	0.399
	336	0.634	0.338	0.635	0.341	0.593	0.390	0.605	0.373	0.517	0.334	0.566	0.376	0.621	0.383	0.583	0.389	0.618	0.328	0.622	0.396
	720	0.640	0.351	0.658	0.349	0.636	0.405	0.645	0.394	0.552	0.352	0.567	0.372	0.626	0.382	0.585	0.391	0.653	0.355	0.632	0.396
	<i>Avg</i>	0.618	0.333	0.627	0.335	0.606	0.395	0.625	0.383	0.529	0.341	0.561	0.373	0.610	0.376	0.581	0.388	0.624	0.340	0.621	0.396
<i>Average</i>	0.574	0.427	0.618	0.442	0.681	0.468	0.686	0.483	0.600	0.436	0.964	0.525	0.701	0.489	0.756	0.491	0.633	0.465	0.662	0.473	

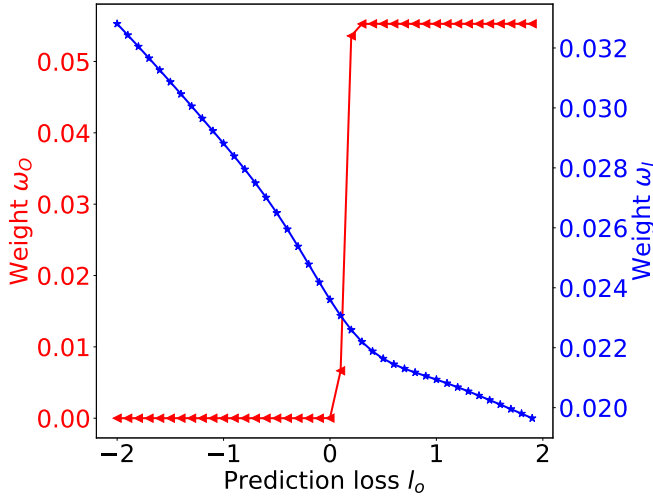


Figure 12: imputation.

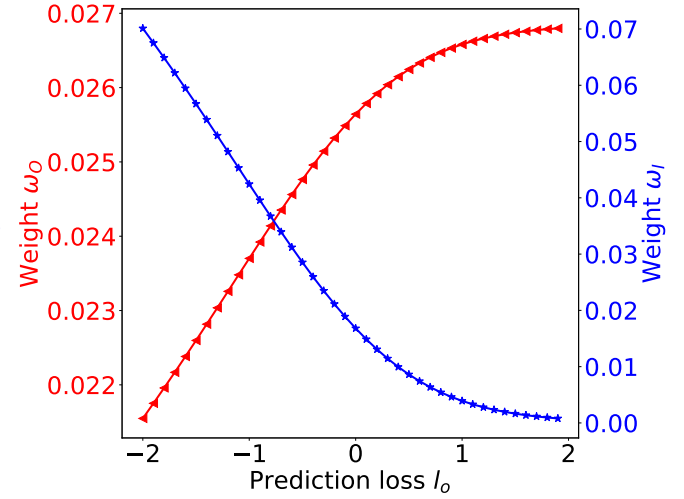


Figure 13: classification

Table 13: Full results for the imputation task. Randomly masked {12.5%, 25%, 37.5%, 50%} of points in 96-length series, averaging results over 4 mask ratios.

Methods	Mask Ratio	LLM-TS		TimesNet		GPT4TS		PatchTST		LightTS		DLinear		FEDformer		Stationary		Autoformer		Reformer	
		MSE	MAE	MSE	MAE	MSE	MAE	MSE	MAE	MSE	MAE	MSE	MAE	MSE	MAE	MSE	MAE	MSE	MAE	MSE	MAE
ETT <sub>m1</sub>	12.5%	0.018	0.088	0.023	0.101	0.018	0.089	0.041	0.130	0.093	0.206	0.080	0.193	0.052	0.166	0.032	0.119	0.046	0.144	0.042	0.146
	25%	0.022	0.097	0.023	0.101	0.023	0.099	0.044	0.135	0.093	0.206	0.080	0.193	0.052	0.166	0.032	0.119	0.046	0.144	0.042	0.146
	37.5%	0.027	0.108	0.029	0.112	0.030	0.112	0.049	0.143	0.113	0.231	0.103	0.219	0.069	0.191	0.039	0.131	0.057	0.161	0.063	0.182
	50%	0.033	0.120	0.035	0.123	0.042	0.131	0.055	0.151	0.134	0.255	0.132	0.248	0.089	0.218	0.047	0.145	0.067	0.174	0.082	0.208
	Avg	0.025	0.103	0.028	0.109	0.028	0.108	0.047	0.140	0.104	0.218	0.093	0.206	0.062	0.177	0.036	0.126	0.051	0.150	0.055	0.166
ETT <sub>m2</sub>	12.5%	0.018	0.079	0.019	0.081	0.019	0.078	0.108	0.239	0.034	0.127	0.062	0.166	0.056	0.159	0.021	0.088	0.023	0.092	0.108	0.228
	25%	0.020	0.085	0.021	0.087	0.021	0.084	0.028	0.099	0.042	0.143	0.085	0.196	0.080	0.195	0.024	0.096	0.026	0.101	0.136	0.262
	37.5%	0.022	0.089	0.023	0.092	0.024	0.090	0.030	0.104	0.051	0.159	0.106	0.222	0.110	0.231	0.027	0.103	0.030	0.108	0.175	0.300
	50%	0.025	0.096	0.025	0.097	0.027	0.098	0.034	0.110	0.059	0.174	0.131	0.247	0.156	0.276	0.030	0.108	0.035	0.119	0.211	0.329
	Avg	0.021	0.087	0.022	0.089	0.023	0.088	0.029	0.102	0.046	0.151	0.096	0.208	0.101	0.215	0.026	0.099	0.029	0.105	0.157	0.280
ETT <sub>h1</sub>	12.5%	0.058	0.165	0.064	0.170	0.043	0.141	0.093	0.201	0.240	0.345	0.151	0.267	0.070	0.190	0.060	0.165	0.074	0.182	0.074	0.194
	25%	0.046	0.143	0.048	0.146	0.056	0.159	0.107	0.217	0.265	0.364	0.180	0.292	0.106	0.236	0.080	0.189	0.090	0.203	0.102	0.227
	37.5%	0.096	0.209	0.098	0.209	0.074	0.182	0.120	0.230	0.296	0.382	0.215	0.318	0.124	0.258	0.102	0.212	0.109	0.222	0.135	0.261
	50%	0.118	0.228	0.116	0.226	0.104	0.214	0.141	0.248	0.334	0.404	0.257	0.347	0.165	0.299	0.133	0.240	0.137	0.248	0.179	0.298
	Avg	0.087	0.198	0.090	0.199	0.069	0.174	0.115	0.224	0.284	0.373	0.201	0.306	0.117	0.246	0.094	0.201	0.103	0.214	0.122	0.245
ETT <sub>h2</sub>	12.5%	0.039	0.131	0.040	0.132	0.041	0.129	0.057	0.152	0.101	0.231	0.100	0.216	0.095	0.212	0.042	0.133	0.044	0.138	0.163	0.289
	25%	0.046	0.143	0.048	0.146	0.046	0.137	0.061	0.158	0.115	0.247	0.127	0.247	0.137	0.258	0.049	0.147	0.050	0.149	0.206	0.331
	37.5%	0.053	0.154	0.055	0.156	0.053	0.148	0.067	0.166	0.126	0.257	0.158	0.276	0.187	0.304	0.056	0.158	0.060	0.163	0.252	0.370
	50%	0.061	0.165	0.061	0.165	0.060	0.160	0.073	0.174	0.136	0.268	0.183	0.299	0.232	0.341	0.065	0.170	0.068	0.173	0.316	0.419
	Avg	0.050	0.148	0.051	0.150	0.050	0.144	0.065	0.163	0.119	0.250	0.142	0.259	0.163	0.279	0.053	0.152	0.055	0.156	0.234	0.352
ECL	12.5%	0.087	0.203	0.090	0.204	0.080	0.194	0.055	0.160	0.102	0.229	0.092	0.214	0.107	0.237	0.093	0.210	0.089	0.210	0.190	0.308
	25%	0.091	0.207	0.092	0.209	0.087	0.203	0.065	0.175	0.121	0.252	0.118	0.247	0.120	0.251	0.097	0.214	0.090	0.203	0.197	0.312
	37.5%	0.095	0.213	0.096	0.213	0.094	0.211	0.076	0.344	0.141	0.273	0.144	0.276	0.136	0.266	0.102	0.220	0.104	0.229	0.203	0.315
	50%	0.101	0.220	0.102	0.221	0.101	0.220	0.091	0.208	0.160	0.293	0.175	0.305	0.158	0.284	0.108	0.228	0.113	0.239	0.210	0.319
	Avg	0.094	0.211	0.095	0.212	0.091	0.207	0.072	0.183	0.131	0.262	0.132	0.260	0.130	0.259	0.100	0.218	0.101	0.225	0.200	0.313
W <sub>weather</sub>	12.5%	0.026	0.048	0.025	0.047	0.027	0.049	0.029	0.049	0.047	0.101	0.039	0.084	0.041	0.107	0.027	0.051	0.026	0.047	0.031	0.076
	25%	0.029	0.055	0.031	0.062	0.030	0.054	0.031	0.053	0.052	0.111	0.048	0.103	0.064	0.163	0.029	0.056	0.030	0.054	0.035	0.082
	37.5%	0.032	0.059	0.034	0.064	0.034	0.062	0.035	0.058	0.058	0.121	0.057	0.117	0.107	0.229	0.033	0.062	0.032	0.060	0.040	0.091
	50%	0.033	0.061	0.035	0.062	0.037	0.066	0.038	0.063	0.065	0.133	0.066	0.134	0.183	0.312	0.037	0.068	0.037	0.067	0.046	0.099
	Avg	0.030	0.056	0.031	0.059	0.032	0.058	0.060	0.144	0.055	0.117	0.052	0.110	0.099	0.203	0.032	0.059	0.031	0.057	0.038	0.087

Table 14: Complete classification task results. \*, in the Transformers indicates the name of \*former.

Methods	Classical		RNN		TCN	Transformers										MLP		TimesNet	LLM		
	XGB	Roc	LSTNet	LSSL		Trans.	Re.	In.	Pyra.	Auto.	Station.	FED.	ETS.	Flow.	DL	LTS.	GPT4TS		TEST	LLM-TS	
Ethanol	43.7	45.2	39.9	31.1	28.9	32.7	31.9	31.6	30.8	31.6	32.7	31.2	28.1	33.8	32.6	29.7	30.4	26.2	25.1	31.9	
FaceD	63.3	64.7	65.7	66.7	52.8	67.3	68.6	67.0	65.7	68.4	68.0	66.0	66.3	67.6	68.0	67.5	68.6	67.8	50.1	68.9	
HandW	15.8	58.8	25.8	24.6	53.3	32.0	27.4	32.8	29.4	36.7	31.6	28.0	32.5	33.8	27.0	26.1	32.1	28.9	20.1	32.7	
HeartB	73.2	75.6	77.1	72.7	75.6	76.1	77.1	80.5	75.6	74.6	73.7	73.7	71.2	77.6	75.1	75.1	77.6	72.2	73.7	77.1	
JapanV	86.5	96.2	98.1	98.4	98.9	98.7	97.8	98.9	98.4	96.2	99.2	98.4	95.9	98.9	96.2	96.2	97.2	98.4	78.4	98.1	
PEMS	98.3	75.1	86.7	86.1	68.8	82.1	82.7	81.5	83.2	82.7	87.3	80.9	86.0	83.8	75.1	88.4	89.6	79.2	59.5	90.8	
SCP1	84.6	90.8	84.0	90.8	84.6	92.2	90.4	90.1	88.1	84.0	89.4	88.7	89.6	92.5	87.3	89.8	90.4	90.1	84.0	91.8	
SCP2	48.9	53.3	52.8	52.2	55.6	53.9	56.7	53.3	53.3	50.6	57.2	54.4	55.0	56.1	50.5	51.1	57.1	50.0	54.4	57.8	
SpokenA	69.6	71.2	100.0	100.0	95.6	98.4	97.0	100.0	99.6	100.0	100.0	100.0	100.0	98.8	81.4	100.0	98.6	97.9	82.1	98.6	
UWave	75.9	94.4	87.8	85.9	88.4	85.6	85.6	85.6	83.4	85.9	87.5	85.3	85.0	86.6	82.1	80.3	85.5	85.9	84.4	86.6	
Avg	66.0	72.5	71.8	70.9	70.3	71.9	71.5	72.1	70.8	71.1	72.7	70.7	71.0	73.0	67.5	70.4	72.7	69.5	61.2	73.4	

Table 15: Full results for the anomaly detection.

Methods	Metrics	SMD			MSL			SMAP			SWaT			PSM			Avg F1 %
		P	R	F1													
LLM-TS		88.09	81.54	84.69	89.04	74.49	81.11	89.95	56.51	69.41	91.16	95.40	93.23	98.44	96.45	97.43	85.17
TimesNet		87.93	81.45	84.57	88.62	73.48	80.34	89.59	56.35	69.18	91.00	95.33	93.12	98.40	96.18	97.27	84.90
GPT4TS		87.70	81.19	84.32	82.15	81.32	81.73	90.04	55.75	68.86	92.12	93.06	92.59	98.37	96.34	97.34	84.97
PatchTST		87.26	82.14	84.62	88.34	70.96	78.70	90.64	55.46	68.82	91.10	80.94	85.72	98.84	93.47	96.08	82.79
ETSformer		87.44	79.23	83.13	85.13	84.93	85.03	92.25	55.75	69.50	90.02	80.36	84.91	99.31	85.28	91.76	82.87
FEDformer		87.95	82.39	85.08	77.14	80.07	78.57	90.47	58.10	70.76	90.17	96.42	93.19	97.31	97.16	97.23	84.97
LightTS		87.10	78.42	82.53	82.40	75.78	78.95	92.58	55.27	69.21	91.98	94.72	93.33	98.37	95.97	97.15	84.23
DLinear		83.62	71.52	77.10	84.34	85.42	84.88	92.32	55.41	69.26	80.91	95.30	87.52	98.28	89.26	93.55	82.46
Stationary		88.33	81.21	84.62	68.55	89.14	77.50	89.37	59.02	71.09	68.03	96.75	79.88	97.82	96.76	97.29	82.08

Table 16: Different traditional models. We use prediction length  $O \in \{96, 192, 336, 720\}$  for ILI and  $O \in \{24, 36, 48, 60\}$  for others.

Methods	PatchTST		PatchTST INT		ETSformer		ETS INT		Stationary		Stat INT		FreTS		FreTS INT		
Metric	MSE	MAE	MSE	MAE	MSE	MAE	MSE	MAE	MSE	MAE	MSE	MAE	MSE	MAE	MSE	MAE	
<i>Weather</i>	96	0.174	0.216	0.172	0.214	0.196	0.282	0.200	0.285	0.178	0.226	0.201	0.246	0.187	0.243	0.179	0.235
	192	0.222	0.258	0.219	0.255	0.282	0.364	0.278	0.361	0.235	0.278	0.238	0.280	0.227	0.274	0.221	0.278
	336	0.280	0.298	0.279	0.298	0.344	0.409	0.322	0.382	0.327	0.339	0.312	0.329	0.281	0.325	0.276	0.320
	720	0.356	0.349	0.356	0.348	0.430	0.472	0.427	0.470	0.387	0.383	0.386	0.383	0.352	0.382	0.344	0.376
	Avg	0.258	0.280	0.257	0.279	0.313	0.382	0.307	0.375	0.282	0.307	0.284	0.309	0.262	0.306	0.255	0.302
<i>ETTh1</i>	96	0.381	0.398	0.382	0.401	0.554	0.536	0.550	0.532	0.534	0.499	0.523	0.486	0.398	0.412	0.395	0.409
	192	0.421	0.426	0.422	0.428	0.686	0.619	0.690	0.621	0.639	0.560	0.609	0.560	0.454	0.449	0.455	0.451
	336	0.464	0.449	0.460	0.441	0.869	0.730	0.868	0.728	0.790	0.648	0.780	0.634	0.512	0.483	0.502	0.474
	720	0.527	0.500	0.510	0.496	1.085	0.849	1.054	0.830	0.706	0.620	0.701	0.606	0.572	0.547	0.560	0.530
	Avg	0.448	0.443	0.444	0.442	0.799	0.684	0.791	0.678	0.667	0.582	0.653	0.572	0.484	0.473	0.478	0.466
<i>ETTm1</i>	96	0.332	0.368	0.332	0.372	0.526	0.495	0.424	0.434	0.417	0.417	0.412	0.410	0.340	0.375	0.339	0.374
	192	0.368	0.388	0.367	0.388	0.565	0.538	0.458	0.461	0.446	0.437	0.445	0.435	0.395	0.408	0.384	0.399
	336	0.397	0.405	0.396	0.405	0.658	0.603	0.537	0.519	0.582	0.507	0.570	0.491	0.431	0.433	0.420	0.423
	720	0.457	0.445	0.460	0.446	0.801	0.696	0.802	0.696	0.661	0.546	0.660	0.546	0.494	0.470	0.484	0.462
	Avg	0.389	0.402	0.389	0.403	0.638	0.583	0.555	0.528	0.527	0.477	0.522	0.471	0.415	0.422	0.407	0.415
<i>ILI</i>	24	2.229	0.894	2.172	0.856	4.043	1.410	3.607	1.305	2.722	1.024	1.905	0.872	3.226	1.231	3.202	1.213
	36	2.330	0.925	2.347	0.978	3.809	1.358	3.705	1.315	3.026	1.071	2.790	1.068	3.363	1.259	3.000	1.173
	48	2.140	0.894	1.984	0.869	3.851	1.351	3.714	1.309	2.622	1.032	2.132	0.900	3.456	1.285	3.132	1.213
	60	2.037	0.912	1.770	0.831	3.983	1.349	3.935	1.350	2.520	1.035	1.991	0.901	3.749	1.340	3.298	1.243
	Avg	2.184	0.906	2.068	0.884	3.922	1.367	3.740	1.320	2.722	1.041	2.205	0.935	3.449	1.279	3.158	1.211

Table 17: Different LLM embeddings. We use prediction length  $O \in \{96, 192, 336, 720\}$  for ILI and  $O \in \{24, 36, 48, 60\}$  for others.

Methods	LLM-TS (LLaMA)		LLaMA w/o text		GPT2		BERT		No LLM		
Metric	MSE	MAE	MSE	MAE	MSE	MAE	MSE	MAE	MSE	MAE	
<i>Weather</i>	96	0.166	0.217	0.170	0.218	0.168	0.218	0.167	0.217	0.168	0.218
	192	0.229	0.269	0.227	0.266	0.226	0.267	0.229	0.270	0.227	0.268
	336	0.278	0.302	0.295	0.314	0.292	0.310	0.283	0.305	0.298	0.318
	720	0.354	0.351	0.360	0.354	0.359	0.354	0.360	0.354	0.361	0.356
	Avg	0.257	0.285	0.263	0.288	0.261	0.287	0.260	0.287	0.264	0.290
<i>ETTh1</i>	96	0.403	0.420	0.409	0.427	0.408	0.426	0.402	0.421	0.402	0.422
	192	0.440	0.441	0.445	0.445	0.442	0.444	0.452	0.450	0.459	0.455
	336	0.471	0.457	0.490	0.472	0.487	0.467	0.494	0.472	0.471	0.457
	720	0.503	0.487	0.518	0.496	0.517	0.494	0.520	0.497	0.535	0.507
	Avg	0.454	0.451	0.465	0.460	0.464	0.458	0.467	0.460	0.467	0.460
<i>ETTm1</i>	96	0.329	0.371	0.350	0.387	0.338	0.370	0.340	0.375	0.341	0.377
	192	0.380	0.398	0.383	0.398	0.392	0.404	0.401	0.408	0.404	0.413
	336	0.418	0.425	0.423	0.426	0.416	0.423	0.414	0.421	0.432	0.428
	720	0.476	0.440	0.467	0.449	0.477	0.454	0.470	0.445	0.468	0.449
	Avg	0.401	0.409	0.406	0.415	0.406	0.413	0.406	0.412	0.411	0.417
<i>ILI</i>	24	1.921	0.898	1.998	0.929	1.997	0.929	1.917	0.915	2.170	0.947
	36	2.151	0.933	2.422	0.957	2.333	0.958	2.431	1.004	2.093	0.889
	48	2.062	0.892	2.198	0.964	2.269	0.937	2.333	0.961	2.418	0.959
	60	1.759	0.853	2.072	0.948	2.077	0.921	2.089	0.926	2.203	0.971
	Avg	1.973	0.894	2.173	0.950	2.169	0.936	2.193	0.952	2.221	0.942

Table 18: Static Weighting Scheme with Different ratios.

Ratio	0.0		0.2		0.4		0.6		0.8		1.0		Ours	
Metric	MSE	MAE												
<i>ETTh1</i>	0.478	0.468	0.471	0.459	0.465	0.462	0.470	0.463	0.473	0.450	0.471	0.463	0.454	0.451
<i>ETTm1</i>	0.415	0.417	0.408	0.414	0.405	0.412	0.406	0.412	0.417	0.419	0.416	0.419	0.401	0.409